An Analysis of

Project High Water Data

Report No. 03.01
Contract NASW-958
Headquarters
National Aeronautics and
Space Administration

Dr. David D. Woodbridge
Dr. James A. Lasater

March 6, 1965

International Space Corporation
1080 "B" Street
P. O. Box 395
Melbourne, Florida

ABSTRACT

21330

The two Project High Water experiments have produced optical, ELF, radiofrequency, and radar data essential to understanding the effects of data releases of large quantities of water in the ionosphere. Extensive cross correlations were found between the various frequencies of acquired electromagnetic data. These data have been analyzed and a physical model of the expansion process has been developed. Results of the analyses demonstrate that:

(1) Extremely low temperatures will be generated by the evaporation-condensation-sublimation processes. These temperatures will depend upon the type, and quantity of liquid released, and upon the ambient conditions into which the release is made,

(2) The maximum velocity of the expanding ice-water cloud approximated 1.83 km/sec. However, a perturbation wave associated with the liquid release possessed a velocity as high as 3.60 km/sec.,

(3) Considerable turbulence is associated with the sudden release of liquids into space,

(4) Telemetry attenuations can result from inhomogeneous regions within the ionosphere,

(5) Considerable doubt was raised concerning the possible existence of ice in space.

The attenuation effects were found to be both frequency and directionally sensitive. Thus, electromagnetic observations provide a technique for investigating inhomogeneous regions in the ionosphere.

TABLE OF CONTENTS

LIST OF TABLES

1.0 Introduction

In two of the early test flights of Saturn launch vehicles, water was used for ballast in the upper stages to simulate expected future payloads. The second and third stages included one tank each containing 44,000 and 42,000 kg of water, respectively. The tanks were designed to simulate boost phase flight characteristics expected in future missions. In the SA-2 flight, the second stage tank was split longitudinally at an altitude of 105.3 km. The third stage had a series of ports one foot in diameter opened up by primacord discharge (Ref. 1). (This differed from the SA-3 flight, in which both upper stages were split longitudinally at an altitude of 165 km).

Several scientific objectives were considered possible with a High Water experiment (Ref. 2,3,4). These objectives were:

A. Investigate the effect of a large perturbation in the ionosphere.

B. Investigate noctilucent cloud effects.

C. Investigate the behavior of ice in space.

D. Investigate ionospheric wind (Ref. 5).

1.0 Introduction (cont'd)

The SA-2 flight occurred on April 25, 1962, from Cape Canaveral, Florida. A map of the relative locations of the launching site and observation stations is shown in Figure 1.1. Water release was executed at an altitude of 105.3 km and a ground range of approximately 80 km (Ref. 1).

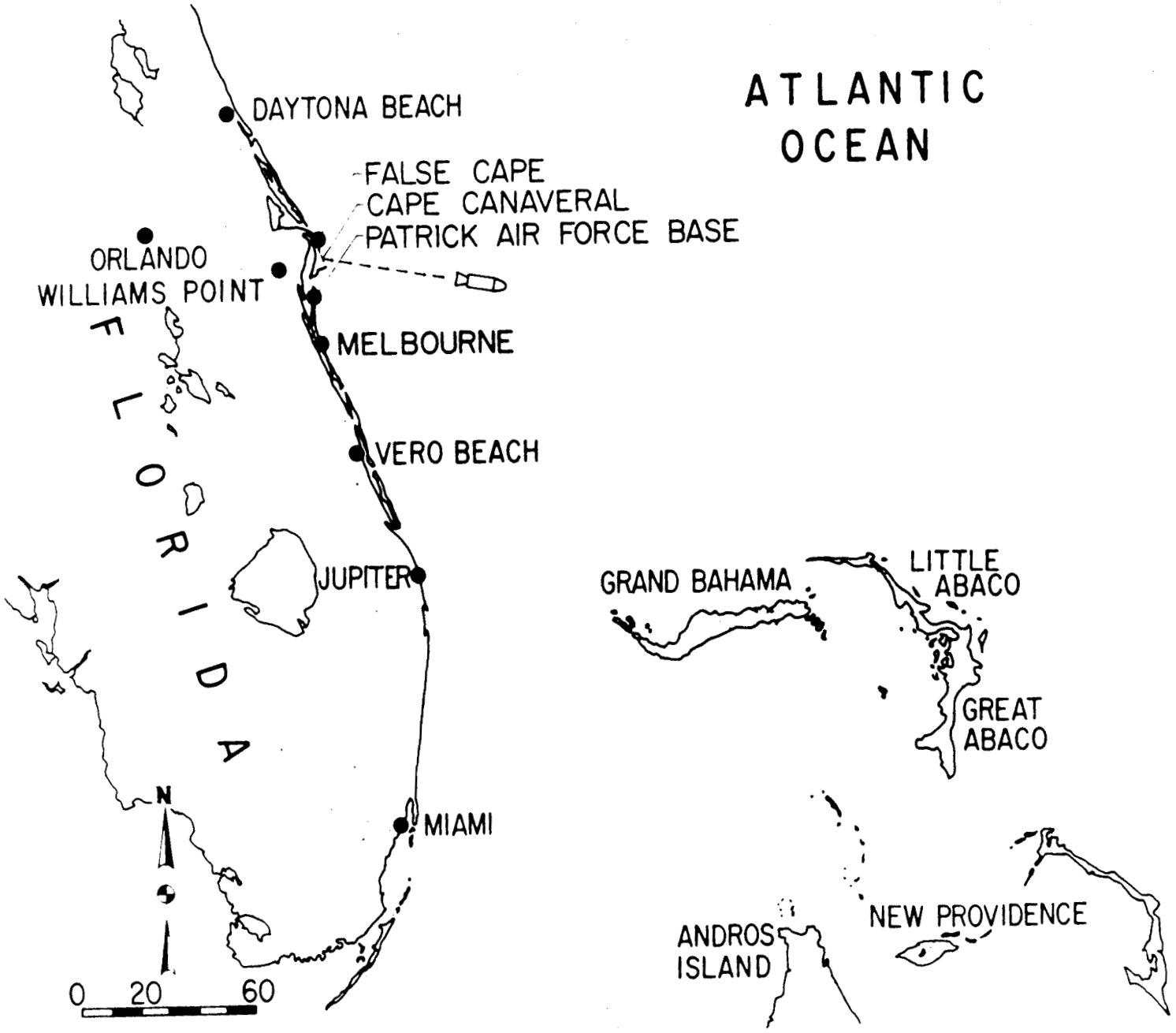

Figure 1.1 Geographical Aera of Project High Water

2.0 Results of Project High Water

Project High Water has proven to be one of the most outstanding experiments yet performed for obtaining direct data on some of the very important physical aspects of the ionosphere and deeper space. This project has yielded the first quantitative data on the effects of releasing large quantities of liquids into the ionosphere, an event that could be caused by rupture of any liquid-carrying space vehicle. In addition to this primary objective of the project, data obtained from the High Water experiments are applicable to a number of other important areas in the development of space research and exploration. Some of the principal contributions of Project High Water to space science are:

1. Generation of a model of the physical processes that occur when large quantities of liquid are released in the near-vacuum of the ionosphere or deeper space,
2. Insight into the physical nature of noctilucent clouds,
3. Support of serious doubts to the theory of the existence of water on the moon,
4. Provision of data raising a number of serious questions concerning the "ice theory" of comets,

2.0 Results of Project High Water (cont'd)

5. Synthetic production of an inhomogeneous region in the ionosphere, providing information, and possible explanations of observed:

   (a) telemetry attenuation, and

   (b) effects of ionospheric perturbations, and

6. Provision of evidence of applicability of ELF spectral observations for the investigation and identification of inhomogeneities in the ionosphere.

The scientific importance and engineering value of the data that can be obtained from fully instrumented Project High Water type experiments should not be underestimated.

3.0 Optical Observations

During the High Water operation optical observations were attempted by:

(a) Direct observation

(b) B.C. 4 cameras

(c) Motion-picture camera

(d) Optical spectrometer

(e) Radiometers

Many of the instruments obtained no data or only partial data. However, some of the motion picture cameras obtained excellent data of the expanding ice-water cloud. The data gathered with the optical spectrometers or radiometers has not been made available.

3.1 Instrumentation

Optical observations of the "High Water" experiments were obtained both from the surface of the earth and from aircraft located at various altitudes and positions. Natural cloud cover blanked observations from some locations, resulting in the loss of spectrographic data except from some airborne instruments. The best optical data was obtained with the 70 mm, 180 inch focal length camera operated from False Cape. A series of frames of the pictures of the expanding ice-water cloud obtained with the False Cape 70 mm camera is shown later on in this section. A complete list of optical instrumentation and the mode of operation of the

3.1 Instrumentation (cont'd)

High Water I experiment (SA-2) is shown in Appendix B. Geographical locations for the principal ground based camera sites are shown in Table 3.1. The coordinates shown in Table 3.1 and the coordinates of the water release (Lat. 28.39413°, Long. 79,74769° and altitude 105.265 km) resulted in the coordinate system for determining the velocity of expansion of the ice-water cloud.

Table 3.1 Station Coordinates

Station	Item No.	Latitude			Longitude			Elevation
		Deg	Min	Sec	Deg	Min	Sec	Feet
False Cape	1.2-64u	28	35	6.4	80	34	43	41
U242L90(Cape Kennedy)	1.2-71u	28	31	28.3	80	34	35	--
Williams Point	1.2-65u	28	26	58	80	45	45	57
Patrick	1.2-67u	28	13	36	80	35	59	38
Melbourne Beach	1.2-68u	28	02	57	80	32	55	39
Vero Beach	1.2-69u	27	40	37	80	21	48	12
Grand Bahama Island West End		26	39	15	78	55	59	5.6
Pelican Point		26	38	33	78	06	48	22.3
Gold Rock Creek		26	36	14	78	22	19	25

3.2 Visual Observations

An excellent chronological recording of the visual behavior of the water release was obtained by Mr. James W. Carter of the Marshall Space Flight Center. Mr. Carter

3.2 Visual Observations (cont'd)

was an observer on an Air Force jet. In a tape recording made at the time of the water release he stated that the aircraft was at flight level 427, about 150 miles due south of Cape Kennedy, with an air speed of 225 knots (Ref. 7). The following description is quoted from Mr. Carter's commentary at the time of the water release.

> "There goes the explosion. Very slight vapor cloud expanding quite rapidly going to about twice the size of the moon. There is a very small dot about the size of a flat pin head and it is now in the process of dissipating. Vapor cloud dissipated very rapidly in about 10 seconds and is completely dissipated at this time. There is still left at the explosion site a very small pin head point of whiteness. There's no reflection, no fluorescence."

Several minutes later, upon reflecting what he had seen, Carter recorded:

> "However, there's one summarizing comment (now) that I have had a little chance to think about it - comparing the size of the vapor cloud to the moon. I originally thought, just from making a rough estimate or instantaneously viewing it, that the vapor cloud expanded (to) about two and a half times the diameter of the moon as I can presently see it. However, on giving this a little more thought it appears as if the could actually expanded to about a diameter of between 4 and 5 inches on the canopy windshield of the cockpit which means it expanded to about 20 times the diameter of the moon and it appeared to be quite circular in all respects. It was not enlongated or elliptical or anything of this nature. It appeared to be quite circular from everything I could see of it."

3.2 Visual Observations (cont'd)

Visual observations were also recorded from G.B.I. (Ref. 8). Five of the G.B.I. station staff observed the water release and the resulting ice-water cloud. Independent written statements obtained from each substantially agreed on the following:

(a) Time of first visual observations: T+164 ± 1 sec.

(b) Duration: 3 - 20 seconds (extreme estimates)
5 seconds (probable value)

(c) Color: white

(d) Brightness: brightness was initially comparable with bright cumulus clouds, decreasing as the cloud diameter increased; perhaps a small dark center

(e) Shape: circular

(f) Growth: very rapid

(g) Size: 2^{o} to 7^{o}

(h) Motion: perhaps some motion along missile trajectory

These reported visual observations are in accord with those obtained in laboratory experiments prior to the High Water Operation (Ref. 6,9). When small quantities of water were suddenly released in a space environment chanber at pressures of 10^{-4} mm Hg the visual observations were only momentary. However, these observations showed an extremely rapid spherical cloud expansion.

3.3 Photographic Analysis

Analysis of the photographs obtained from three different locations shows the time development of the structure of

3.3 Photographic Analysis (Cont'd)

the ice-water cloud. The locations of the stations used for this study of the cloud development, relative to the point of water release, are shown in Figure 3.1. The "y" direction is along the trajectory of the vehicle (Ref. 5).

Figure 3.1 shows that the planes of the observations are nearly perpendicular to each other for the False Cape and Melbourne Beach films. The Vero Beach film shows a slightly more head-on view of the cloud.

As previously mentioned, the best photographs of the water release from the SA-2 vehicle were obtained from False Cape. A series of these pictures is shown in Figures 3.2 through 3.14. Figure 3.2 shows the SA-2 vehicle 12 milliseconds before it was exploded to release the water. The following frame of the motion picture film was exposed 21 milliseconds after the explosion and is shown in Figure 3.3. Several very interesting aspects can be noticed in Figure 3.3. Four faint rays extend from the nearly circular cloud. These rays are distributed uniformly around the cloud. Careful inspection shows a slight haze distributed between these rays. There are also four cloudlets visible within the cloud structure. The cloudlets are also uniformly distributed around the cloud but are offset nearly 30° from the rays. Both the rays shown in Figure 3.3 and the haze are considered to be results of the explosive charge. The denser ring and the system of cloudlets consist of the expanding liquid. This liquid was composed of

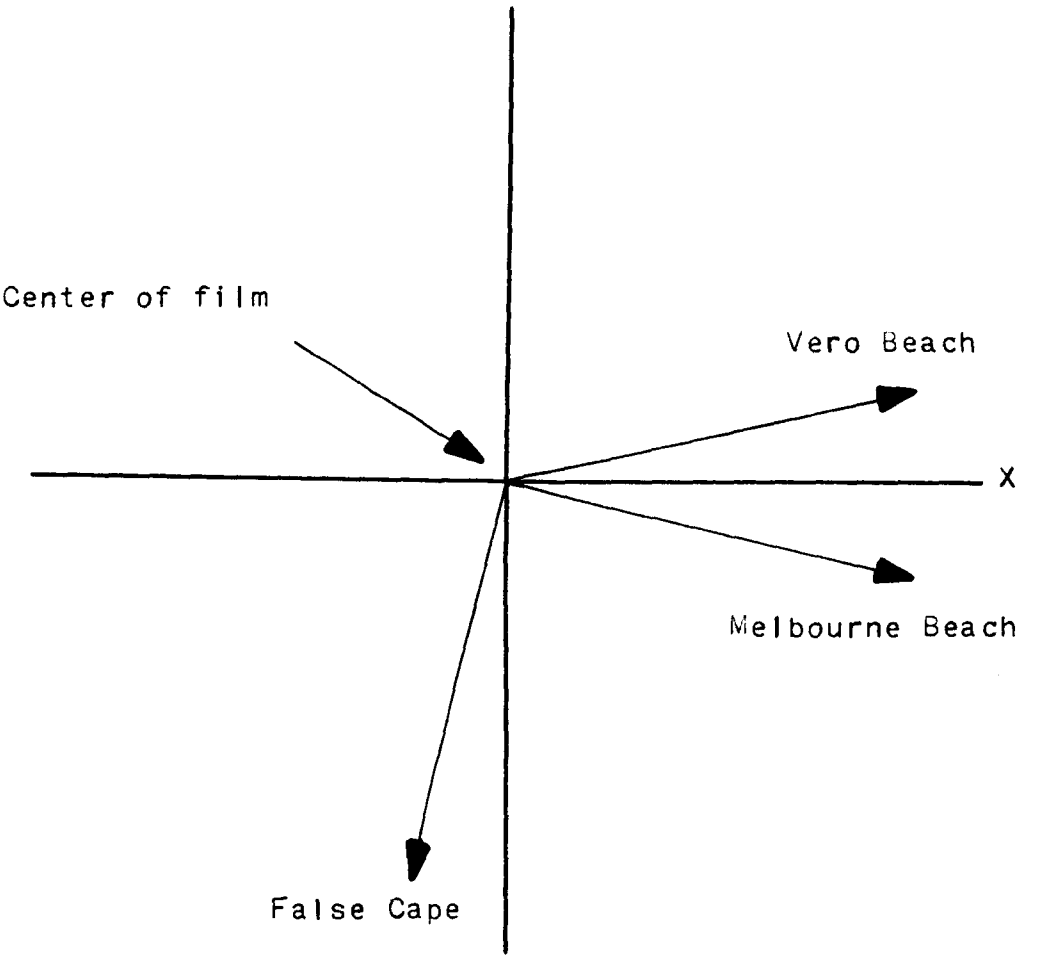

Camera Direction

from the

Ice-Water Cloud

Figure 3.1

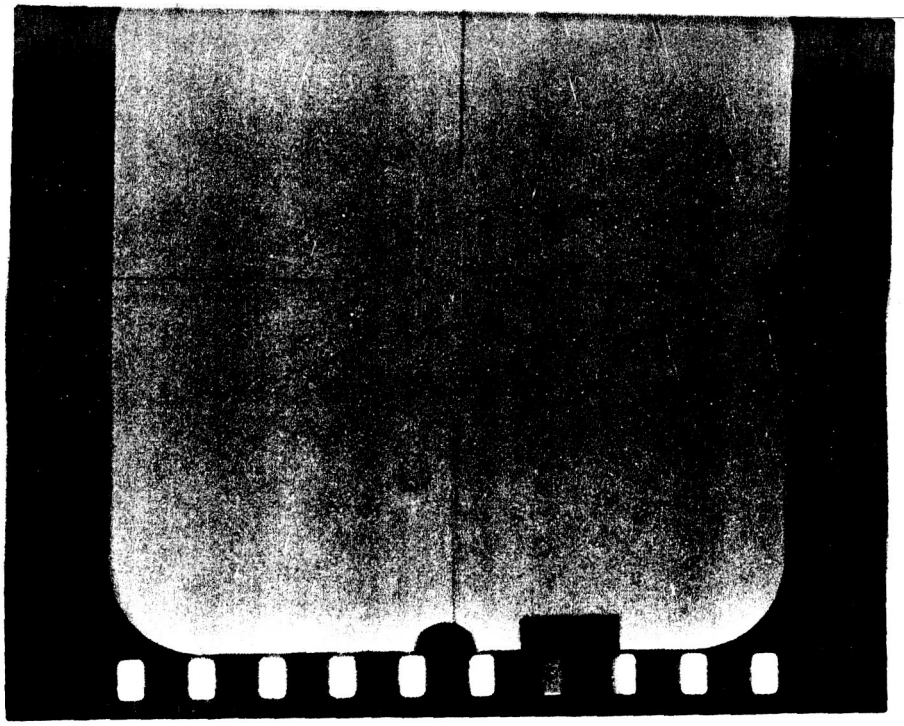

Figure 3.2. SA-2 Launch Vehicle just before Water Release

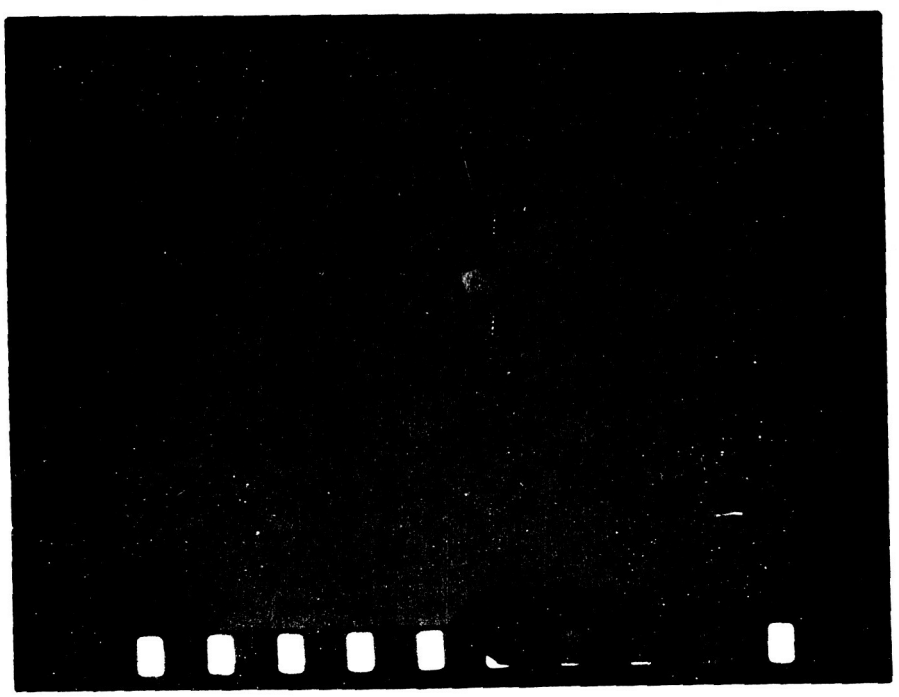

Figure 3.3. Ice-Water Cloud 0.021 Seconds after Release (False Cape)

3.3 Photographic Analysis (cont'd)

44,000 + kg of water, 3,400 kg of fuel (RP-1) and 4,600 kg of liquid oxygen. Laboratory experiments show that these other constituents of the released liquid behave very similarly to water (Ref. 10).

Figure 3.4 shows the expanding cloud 88 milliseconds after the liquid release. All evidence of the four spikes and the haze have disappeared. A rather sharp cloud structure is now evident. The four cloudlets have rotated until they are oriented approximately along the lines of the original spikes. This orientation then remains constant as long as the cloudlets are identifiable. At the time of the liquid release an angular momentum was imparted to the launch vehicle and also to the escaping liquid. (Ref. 5). Thus the rotation of the four cloudlets and the subsequent stabilization demonstrates the rapidity with which the cloud stabilized with the ambient, except for its internal dispersive and turbulent activities. An internal cloud ring is seen to be forming and several regions of material concentration are observed in Figure 3.4. The motions of two of these cloudlets were analyzed until they dissipated, to obtain their expansion velocities.

Sixty-six (66) milliseconds after the time Figure 3.4 was obtained the clouds were as shown in Figure 3.5. No very significant changes occurred within this time interval. However, the outer limits of the cloud are now more diffuse and the cloud structure more definite. The inner ring is

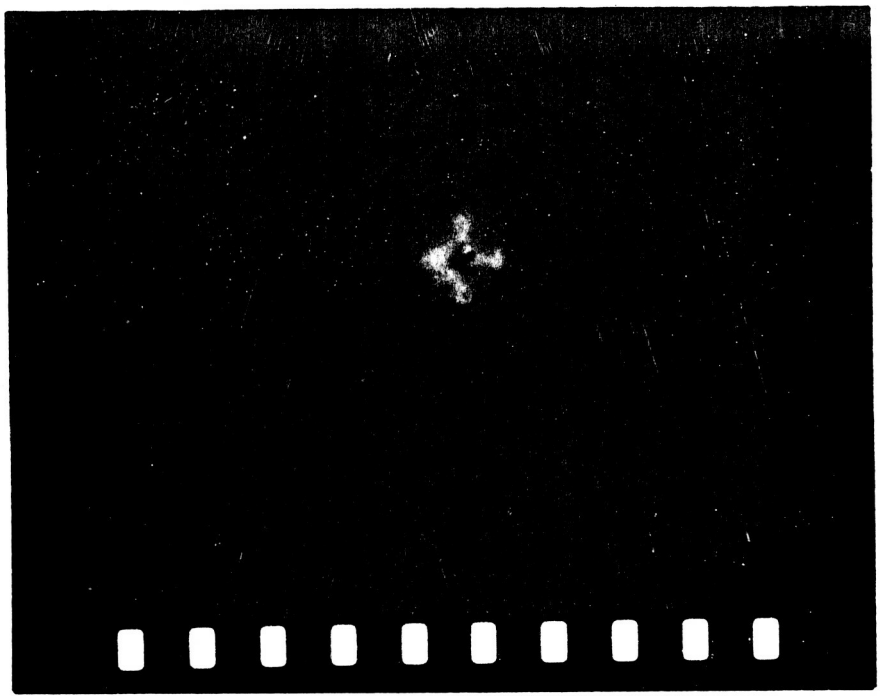

Figure 3.4. Ice-Water Cloud 0.088 Seconds after Release (False Cape)

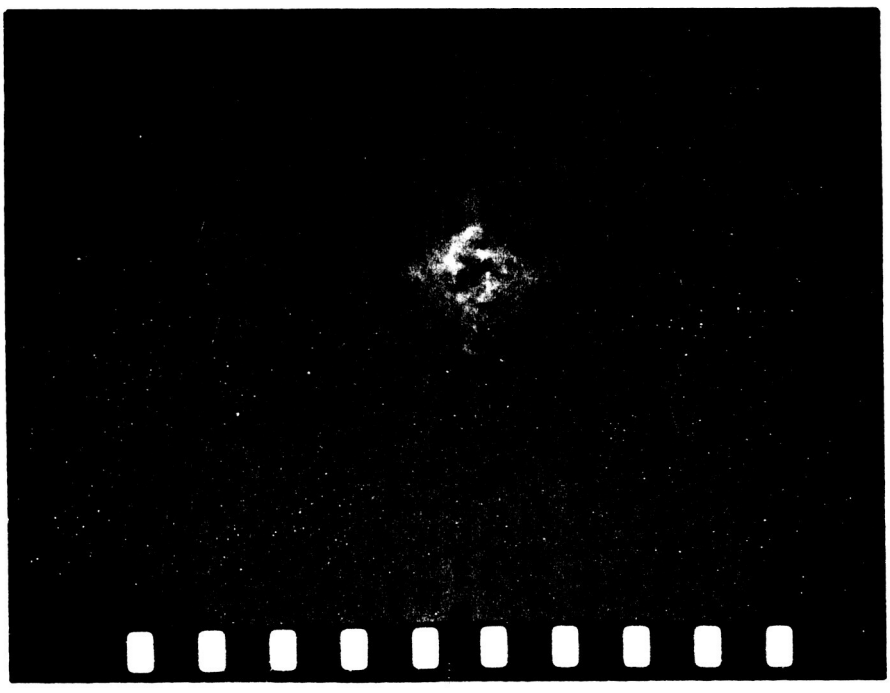

Figure 3.5. Ice-Water Cloud 0.154 Seconds after Release (False Cape)

3.3 Photographic Analysis (cont'd)

now the principal observable feature.

During the following 134 milliseconds the cloud continued to expand as shown in Figures 3.6 and 3.7. One of the interesting aspects of these figures is the increased reflections of the inner cloud structure. Turbulence and condensation effects can now be observed within the structure of the cloud.

Figures 3.8 and 3.9 show the cloud at 454 and 722 milliseconds after the liquid release. A unique feature of Figure 3.8 is the bulge that develops toward the lower right-hand portion of the cloud. This bulge expanded outward much more rapidly than the inner, more reflective portion of the cloud. In both of these figures the effect of turbulence and the condensation-evaporation processes are evident.

By 1.155 seconds after the liquid release, the cloud has begun to expand beyond the field of view of the False Cape camera. This condition is shown in Figure 3.10. The cloudlet structure is very evident in the outer portions of the cloud.

As the cloud structure dissipated, the release of liquid from the third stage of the SA-2 vehicle could be observed. At 4.379 seconds after the first liquid release, the water escaping from the third stage could easily be detected, as shown in Figure 3.11. Figures 3.12, 3.13, and 3.14 show the escaping liquid at 7.845 sec., 10.279 sec.,

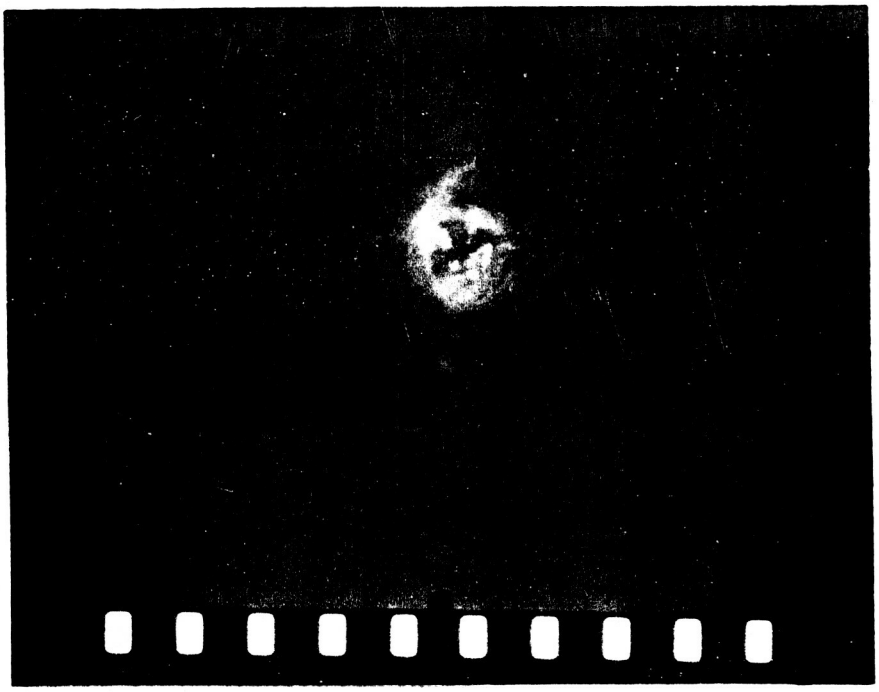

Figure 3.6. Ice-Water Cloud 0.221 Seconds after Release (False Cape)

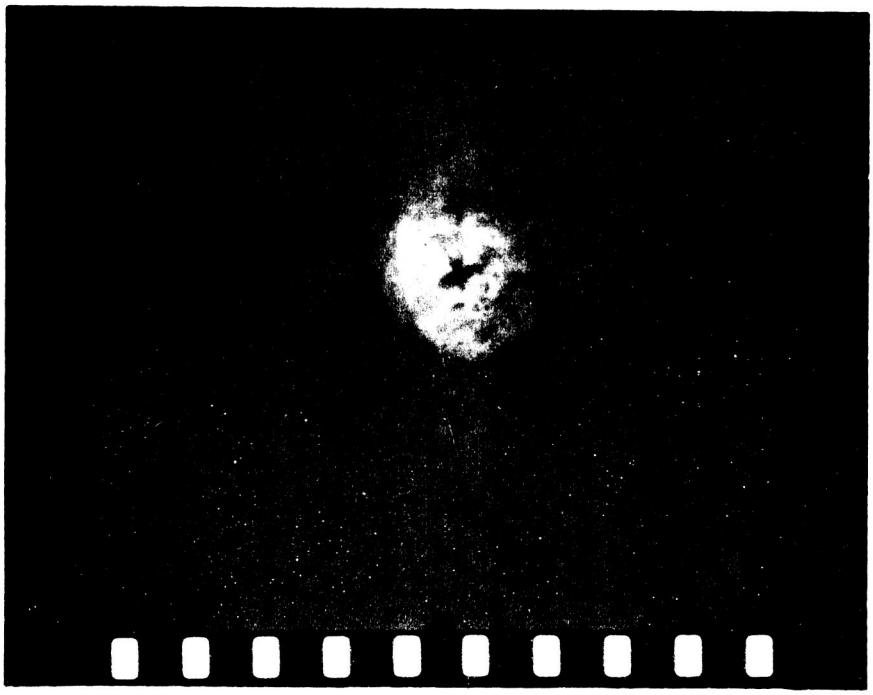

Figure 3.7. Ice-Water Cloud 0.288 Seconds after Release (False Cape)

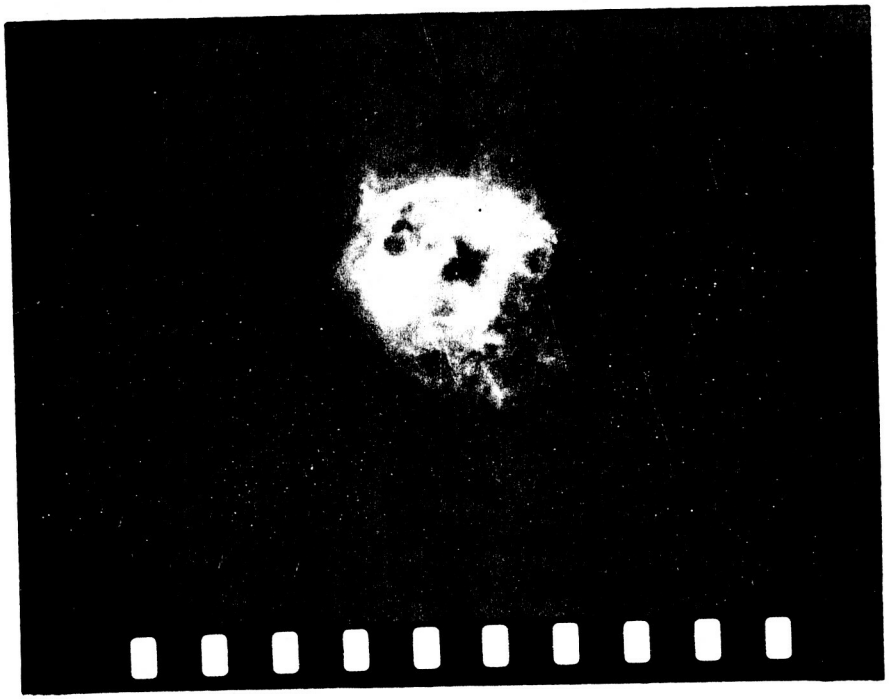

Figure 3.8. Ice-Water Cloud 0.454 Seconds after Release (False Cape)

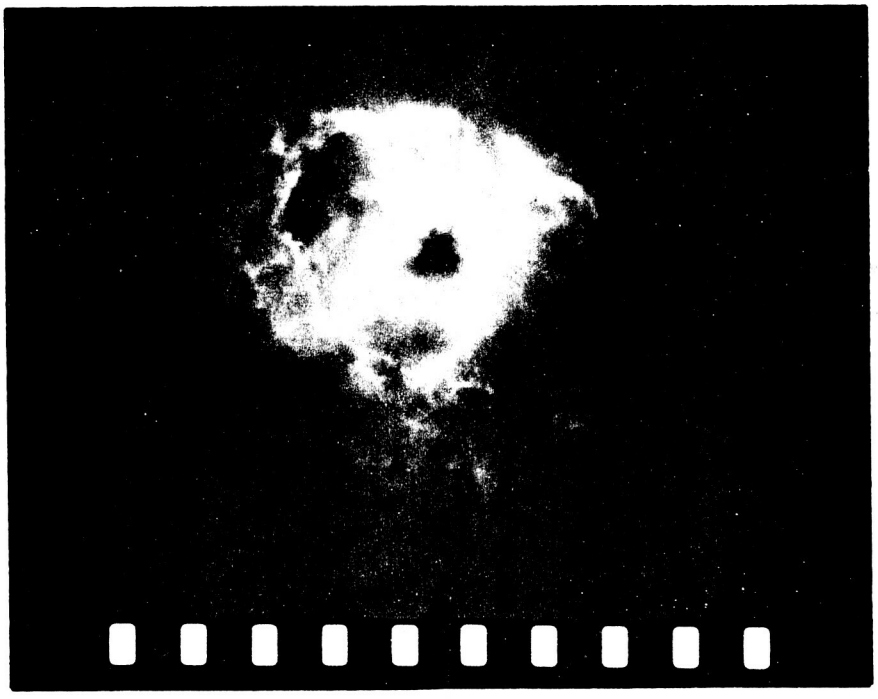

Figure 3.9. Ice-Water Cloud 0.722 Seconds after Release (False Cape)

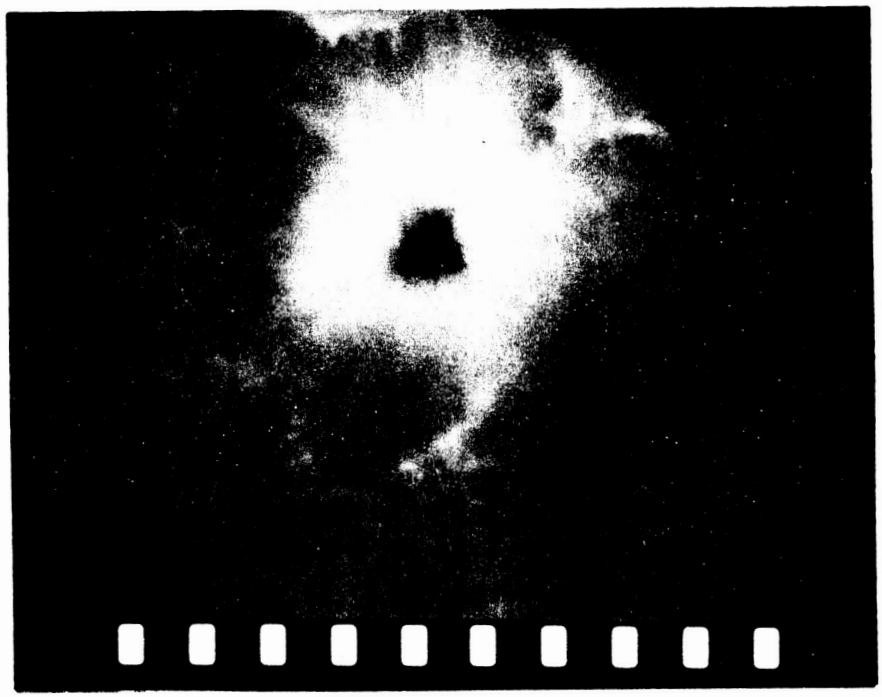

Figure 3.10 Ice-Water Cloud 1.155 Seconds after Release (False Cape)

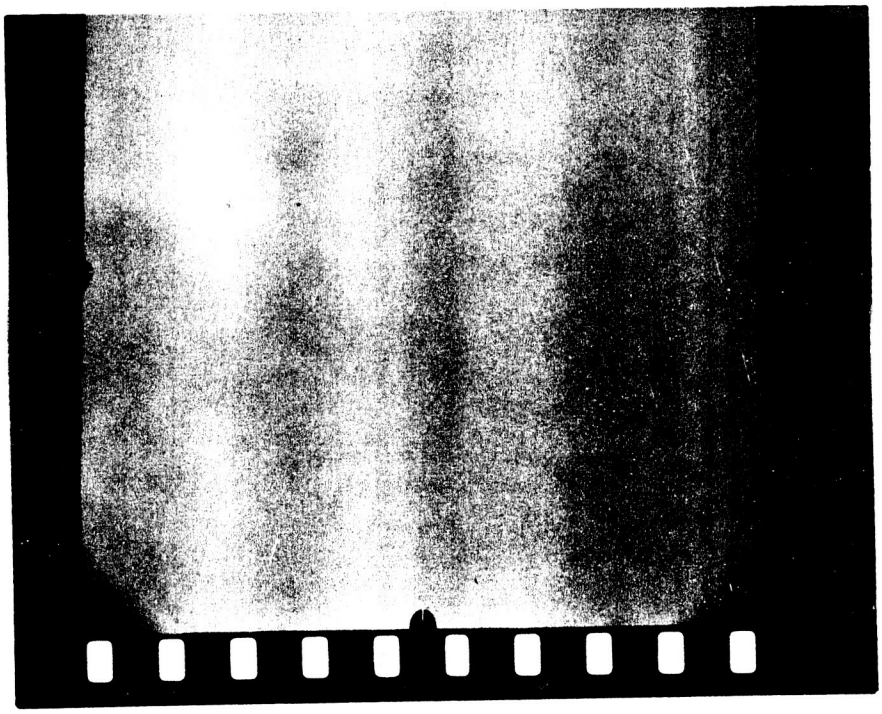

Figure 3.11. Escaping Water from Third Stage at 4.379 Seconds

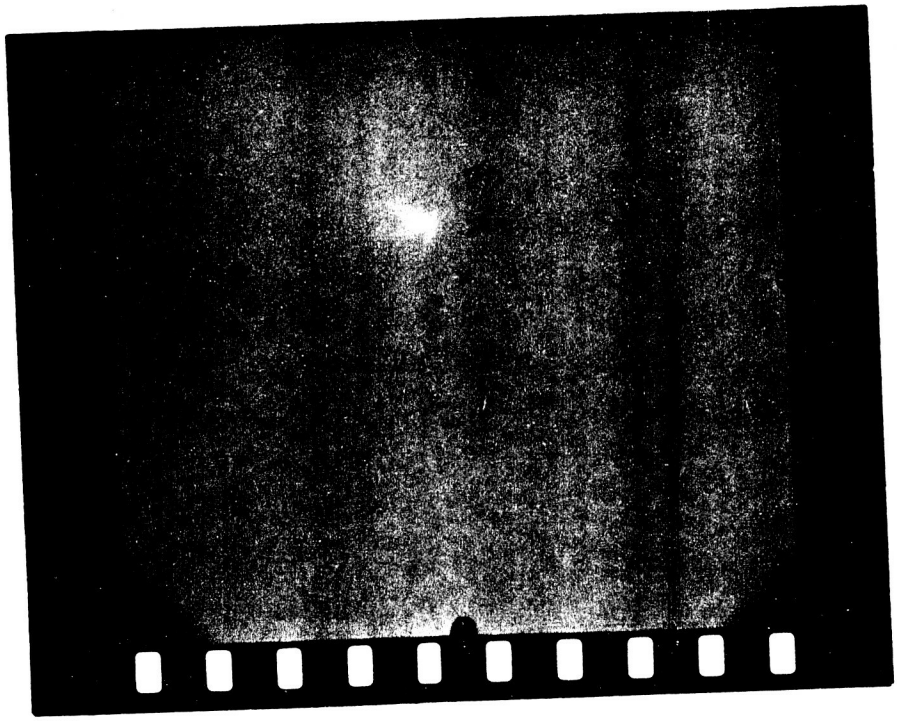

Figure 3.12. Escaping Water from Third Stage at 7.845 Seconds

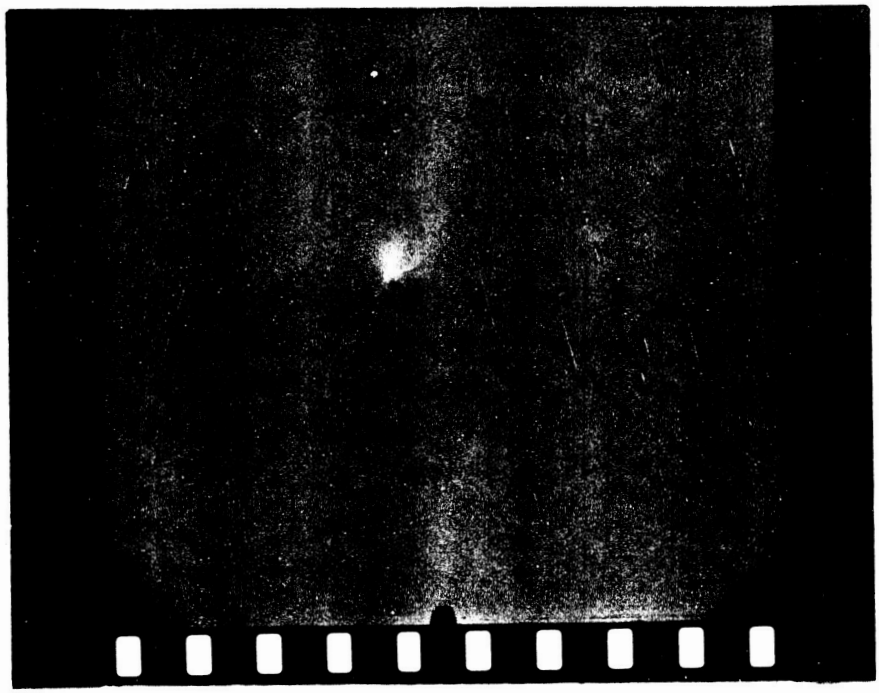

Figure 3.13. Escaping Water from Third Stage at 10.279 Seconds

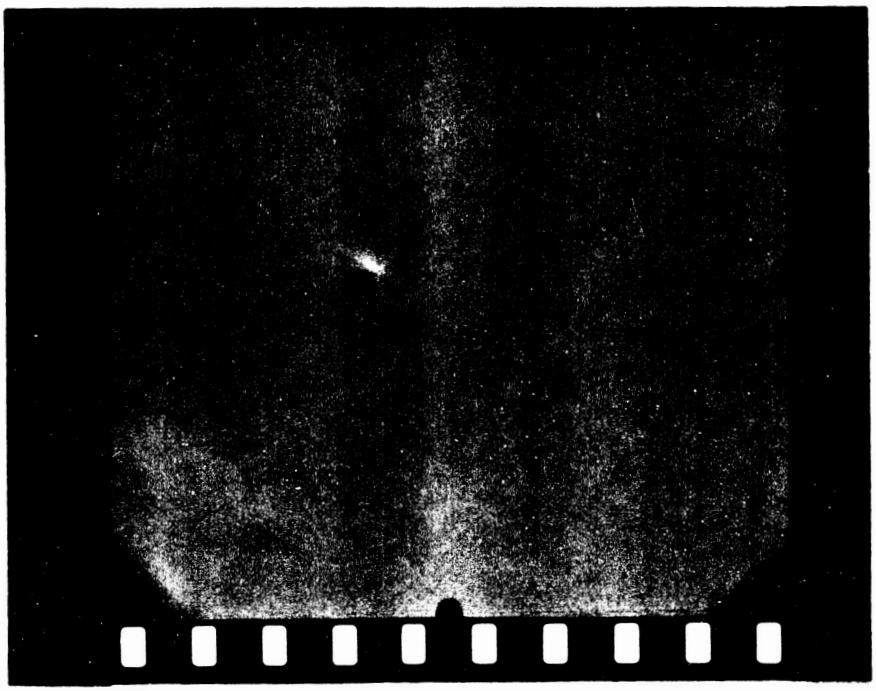

Figure 3.14. Escaping Water from Third Stage at 13.979 Seconds

and 13.979 sec., respectively. Analysis of these figures indicates that the liquid did not flow evenly from the (one foot diameter) ports that were cut in the third stage liquid container. The liquid appears to be discharged in a somewhat random fashion. This condition can be explained by freezing of the liquid being expelled through the ports, followed by melting resulting from conduction of heat from the interior water complicated by evaporation of the ice.

Color pictures of the cloud growth and dissipation were also obtained from Melbourne Beach with a 70 mm, 400 inch focal length camera. The first picture of the expanding cloud, obtained 39 milliseconds after the liquid release, is shown in Figure 3.15. Careful analysis shows the four spikes that were evident in the picture obtained from False Cape at 22 milliseconds after the liquid release. However, the haze in the Melbourne Beach picture can not be resolved. Also the cloud structure is not resolved as it is with the False Cape camera. Figure 3.16 shows the cloud as seen from Melbourne Beach 239 milliseconds after the liquid release. This is only 18 milliseconds after the picture (Figure 3.6) that was taken from False Cape. Comparing these two pictures provides an interesting model of the geometry of the expanding cloud. Remembering that the views of the cloud are nearly at right angles to each other, there appears to be six original cloudlets instead of four. These original cloudlets expand to the four bulges that appear outside the

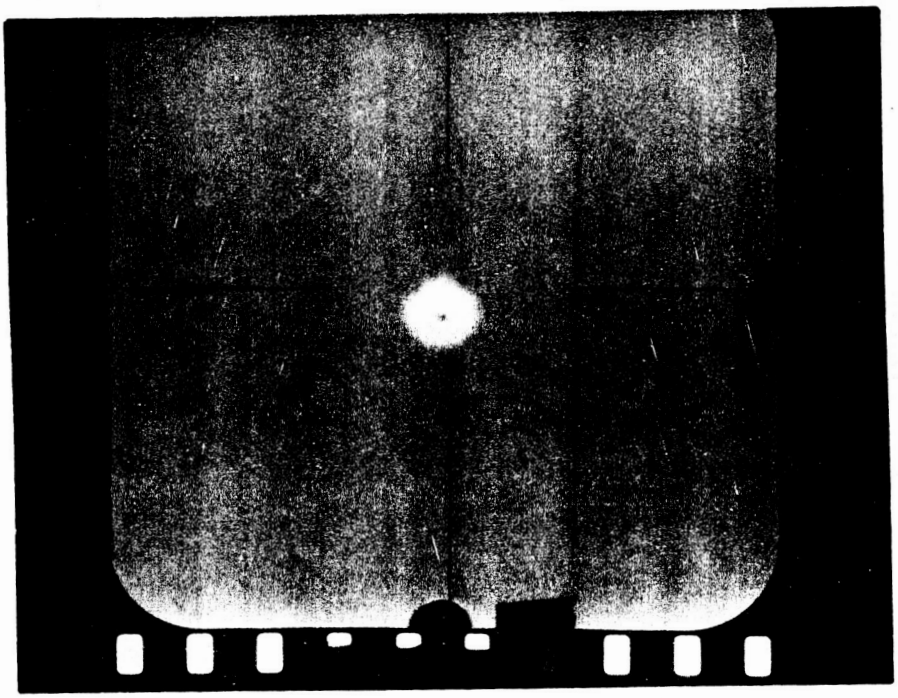

Figure 3.15. Ice-Water Cloud 0.039 Seconds after Release (Melbourne Beach)

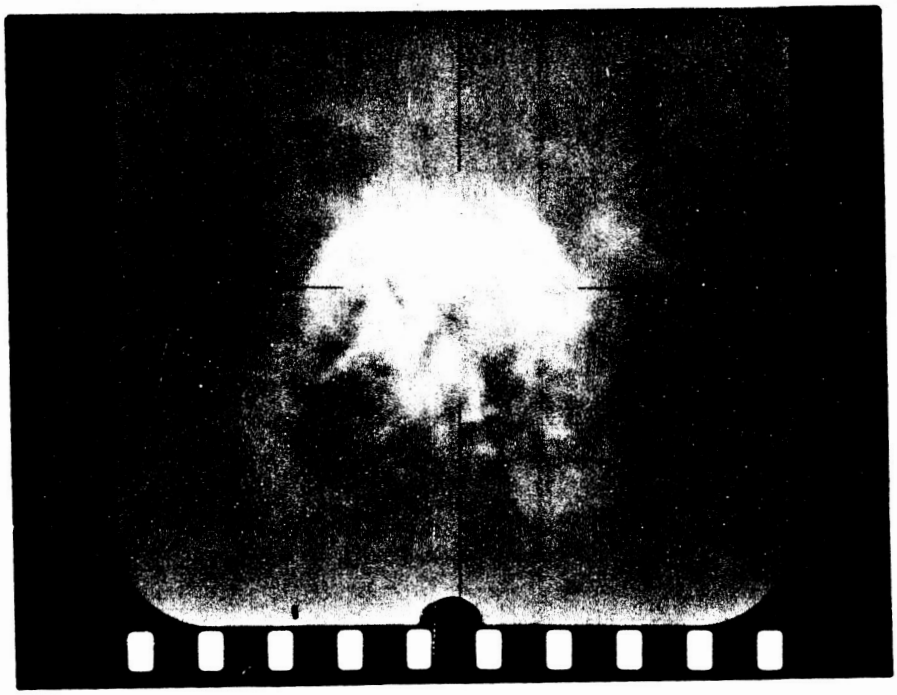

Figure 3.16. Ice-Water Cloud 0.239 Seconds after Release (Melbourne Beach)

3.3 Photographic Analysis (cont'd)

more reflective inner portions of the cloud. The bulges that appear horizontal in Figure 3.6 are directed into and through the cloud, as observed in Figure 3.16.

By 489 milliseconds, the cloud was expanding beyond the field of view of the Melbourne Beach camera, as shown in Figure 3.17. As with the previously discussed picture, the effects of turbulence and the condensation-evaporation process are evident.

As the cloud dissipated, the liquid release from the third stage could be photographed. A series of three photographs obtained at 8.439 sec., 20.939 sec., and 34.739 sec., are shown in Figures 3.18, 3.19, and 3.20. These photographs appear similar to those obtained from False Cape and substantiate the theory of the liquid release from the ports.

A set of pictures of the cloud expansion obtained from Vero Beach is shown in Figure 3.21. The structure detail of the cloud is not comparable to that obtained with the color cameras. However, the shorter focal length camera did provide pictures of the total cloud for a longer period of time. These pictures, from Vero Beach, indicate that after the initial structure dissipated the cloud expanded in nearly a spherical manner.

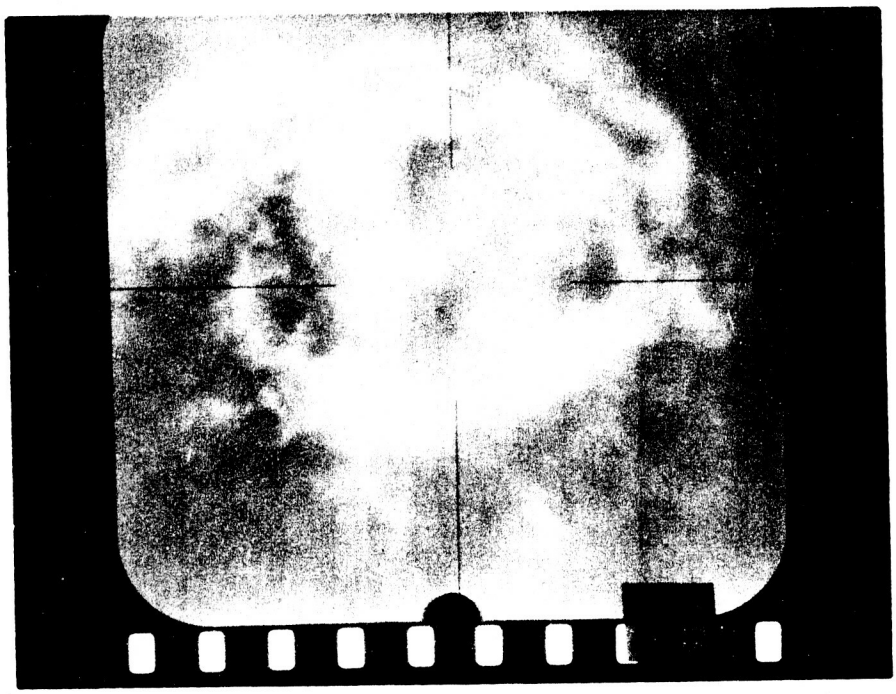

Figure 3.17. Ice-Water Cloud 0.489 Seconds after Release (Melbourne Beach)

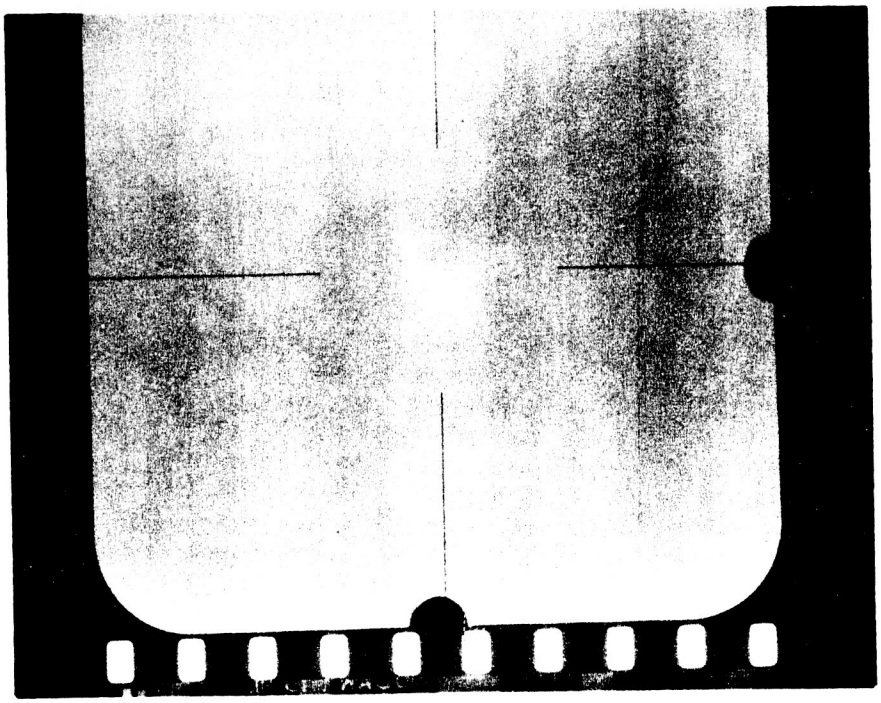

Figure 3.18. Escaping Water from Third Stage at 8.439 Seconds

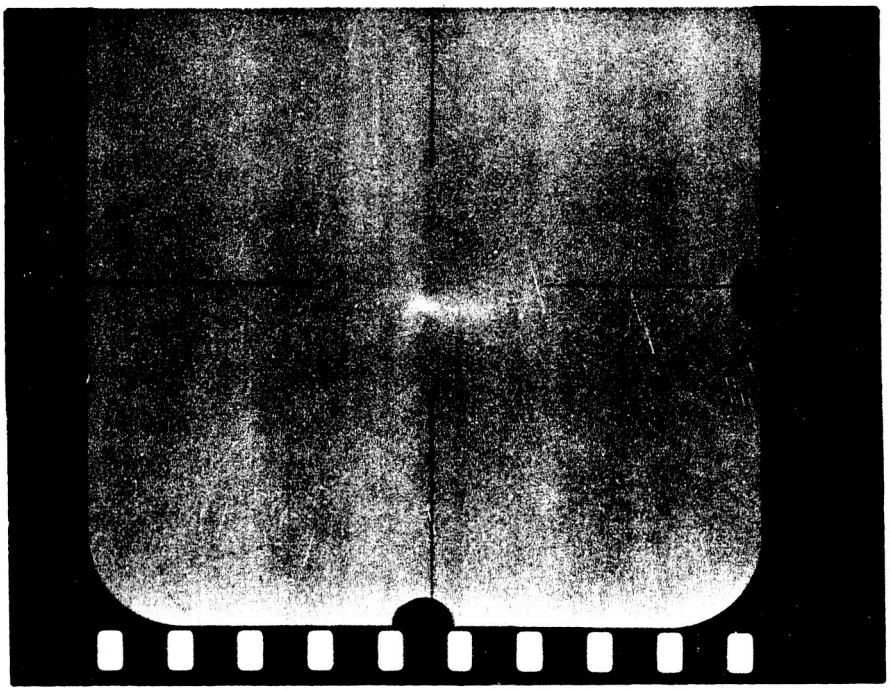

Figure 3.19. Escaping Water from Third Stage at 20.939 Seconds

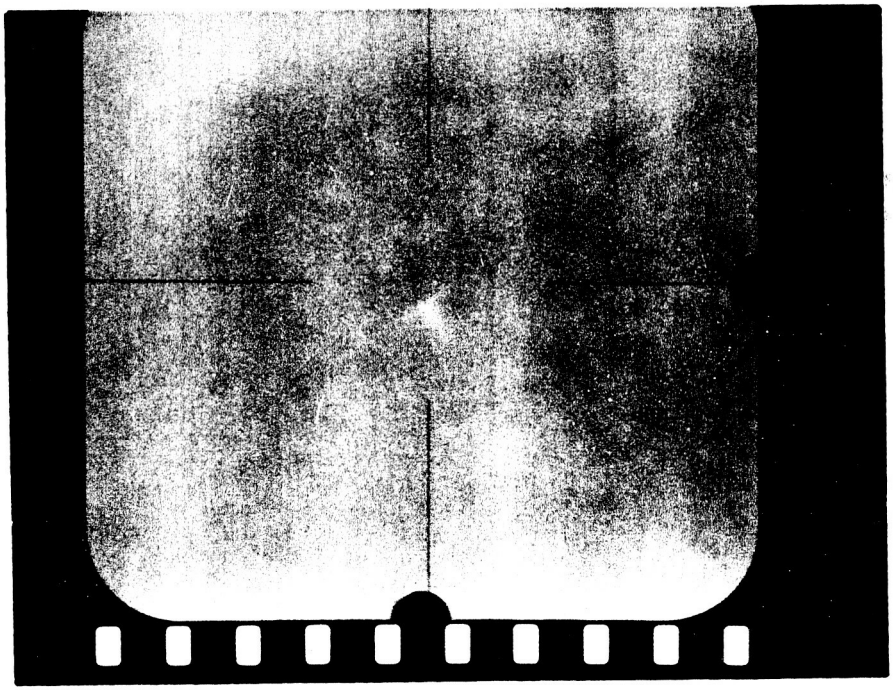

Figure 3.20. Escaping Water from Third Stage at 34.739 Seconds

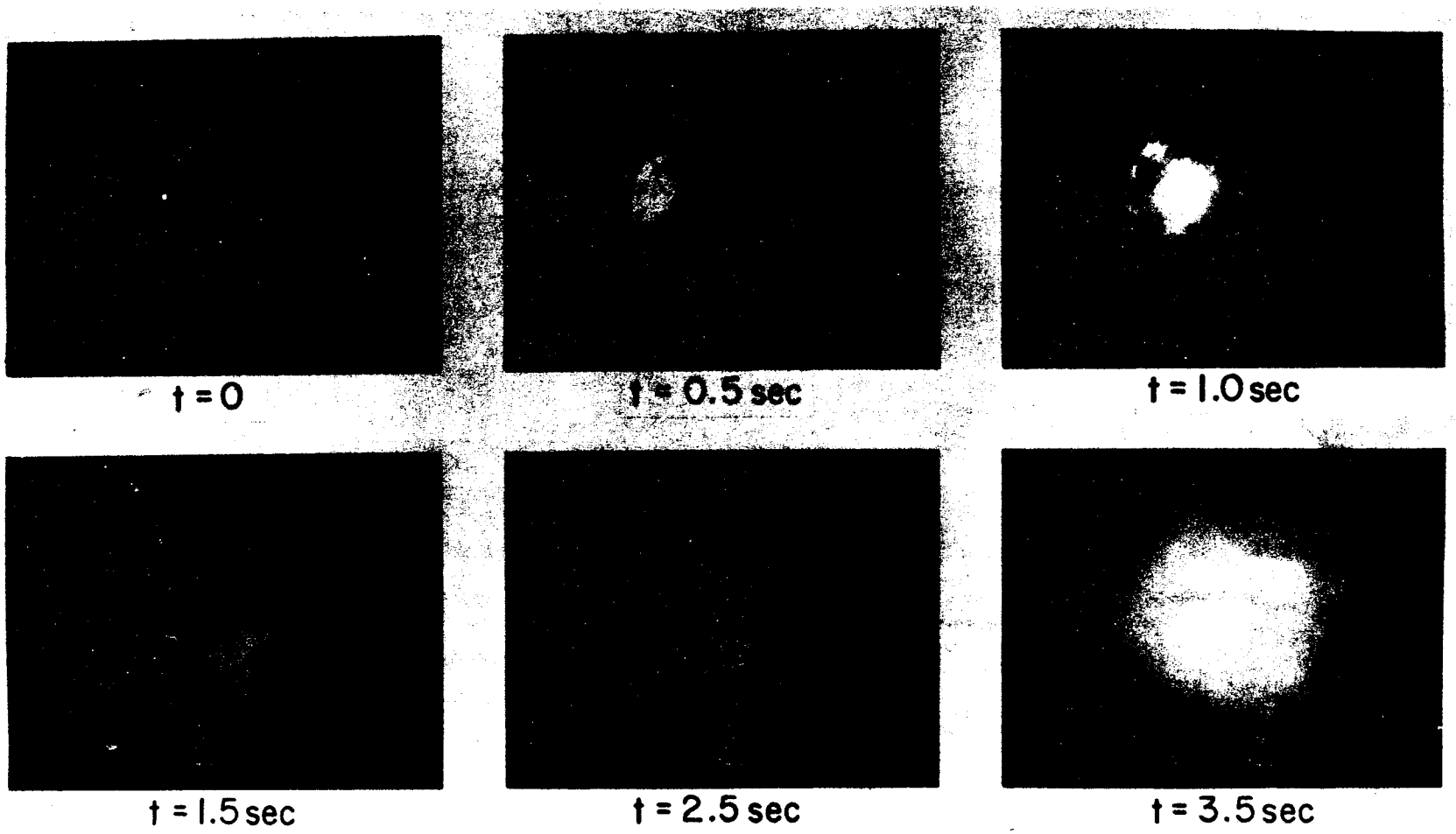

Motion Picture Sequence of SA-2 Water Release Experiment Project "HIGHWATER"
Scale : Horizontal width of frame = 4.15 miles

Figure 3.21

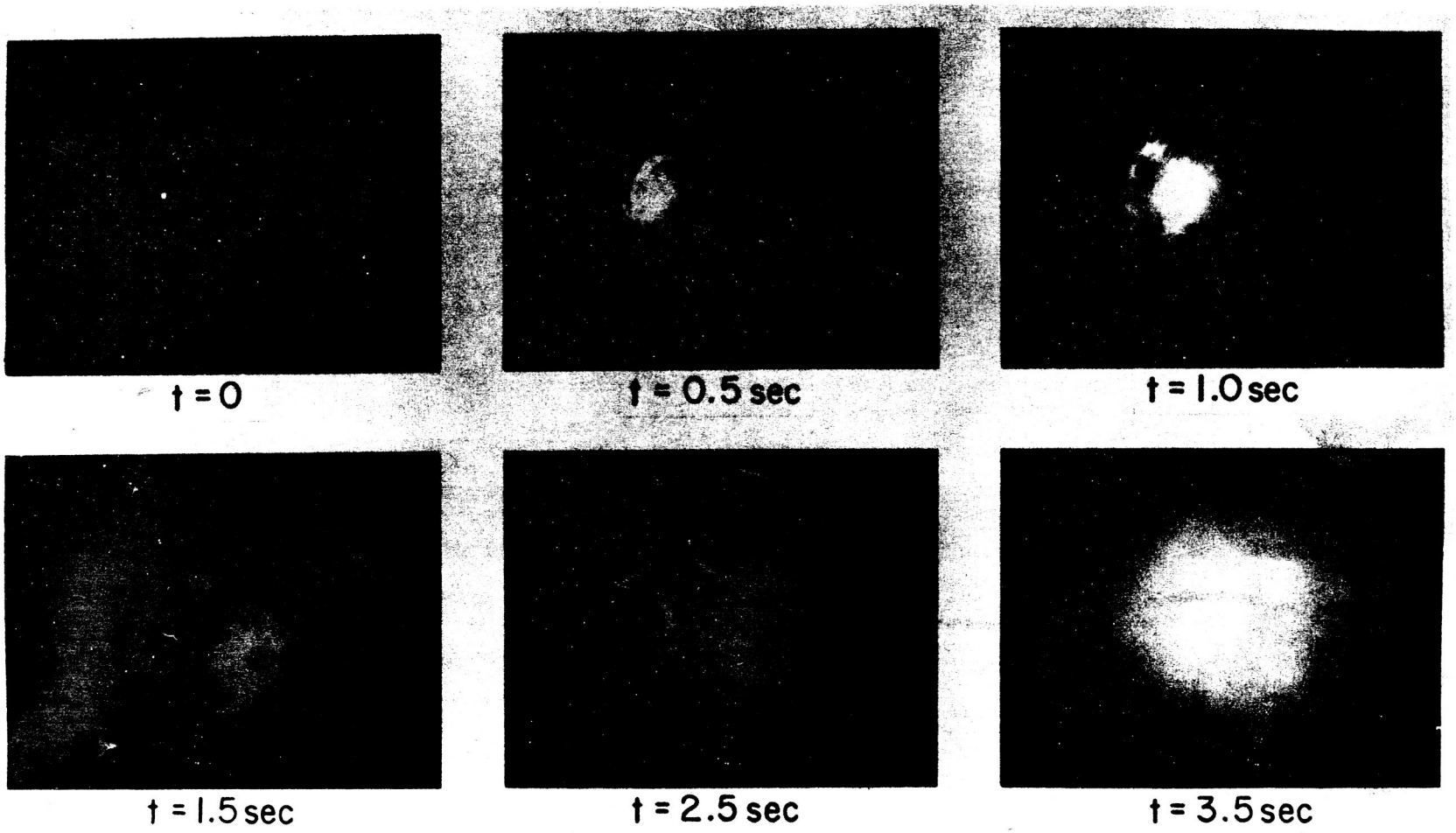

Motion Picture Sequence of SA-2 Water Release Experiment Project "HIGHWATER"
Scale : Horizontal width of frame = 4.15 miles

Figure 3.21

3.4 Expansion Rate Analysis

The expansion of liquids under reduced pressure is a complex phenomena because of the phase changes that occur. A mathematical theory has been developed utilizing hydrodynamic-thermodynamic considerations (See Appendix C). Utilizing these considerations an equation can be developed for the density of the expanding liquid. However, in the cases where rapid phase changes occur experimental data are required to determine the changes that occur in the expansion model.

Cloud expansion velocities were obtained by measuring the actual displacement of the cloud edge, or the center of a particular cloudlet, on a series of frames. The actual distance moved was calculated from the known focal length of the camera, frame size, and distance from the camera location to the cloud.

Expansion velocities of the spikes that appeared on the first picture obtained after the explosion (T+0.021 sec.) are 3.3 km/sec. This velocity is, of course, an average velocity over the first 21 milliseconds. However, this may be a good estimate of the initial perturbation wave velocity.

Expansion velocities were measured for the outer and inner cloud systems and the radial velocities were measured for six distinctive cloudlets. The velocities of the various cloud forms are shown in Figure 3.22. Fluctuation in the velocities with time are due to turbulence and condensation-evaporation dynamics within the cloud. It is of interest to

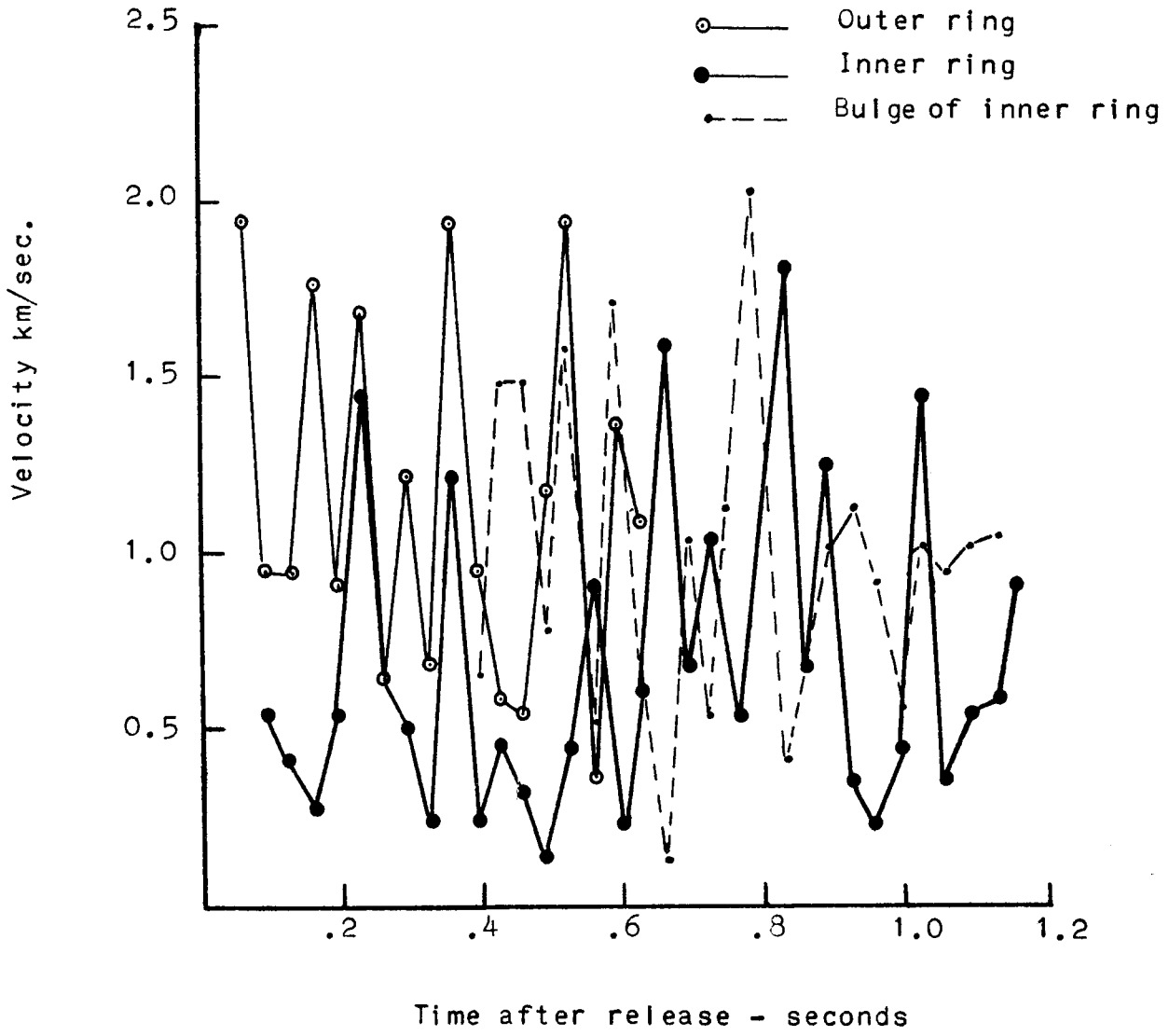

Velocities of the Edges of the Cloud (False Cape)

Figure 3.22

3.4 Expansion Rate Analysis (cont'd)

note that the outer ring had an average velocity considerably greater than the inner ring. When the bulge developed in the inner ring, its average velocity was greater than the cloud region from which it developed, but not as great as the outer ring velocity. Fluctuations in the velocity of this bulge appeared to damp out as it expanded beyond the field of view of the camera. However, the fluctuations in the velocity of the inner ring continued.

Figure 3.23 shows the velocities of three of the six cloudlets as a function of time, while Figure 3.24 shows the velocities of the remaining three cloudlets. Cloudlet number one was embedded in the outer ring of the expanding vapor. Correspondingly, the average velocity of this cloudlet is nearly the same as that of the outer ring, while the velocities of the other cloudlets are closer to the average velocity of the inner ring. As with the cloud expansion velocities, the cloudlet velocities fluctuated due to the turbulence and due to the energy imbalance produced by the complex condensation-evaporation process taking place within the cloud.

Pictures obtained from the Melbourne Beach camera location also provided cloud expansion velocity calculations. These velocities as a function of time are shown in Figure 3.25. The longer focal length camera did not permit the

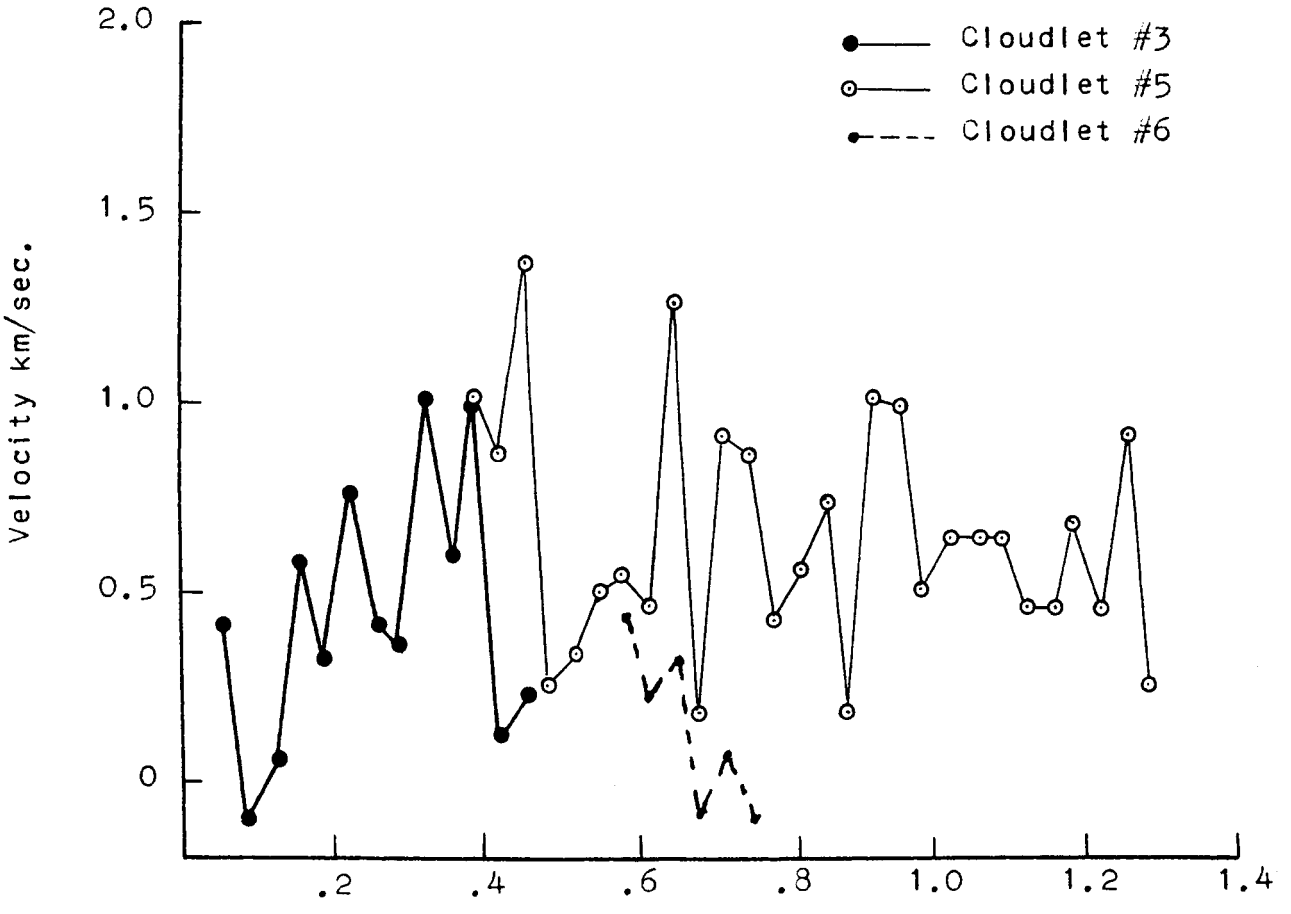

Velocities of Cloudlets within the Cloud Structure
(False Cape)

Figure 3.23

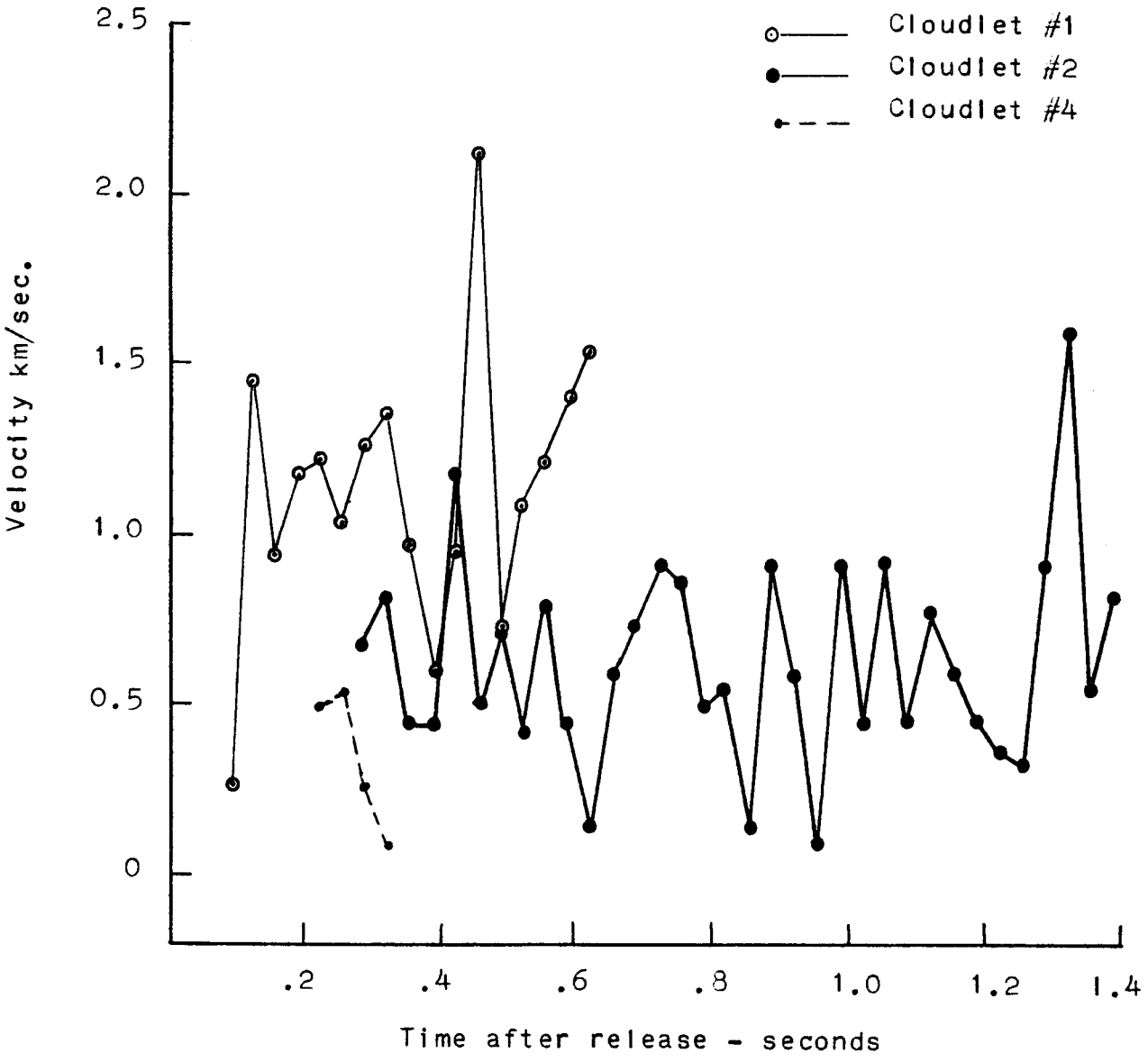

Velocities of Cloudlets within the Cloud Structure (False Cape)

Figure 3.24

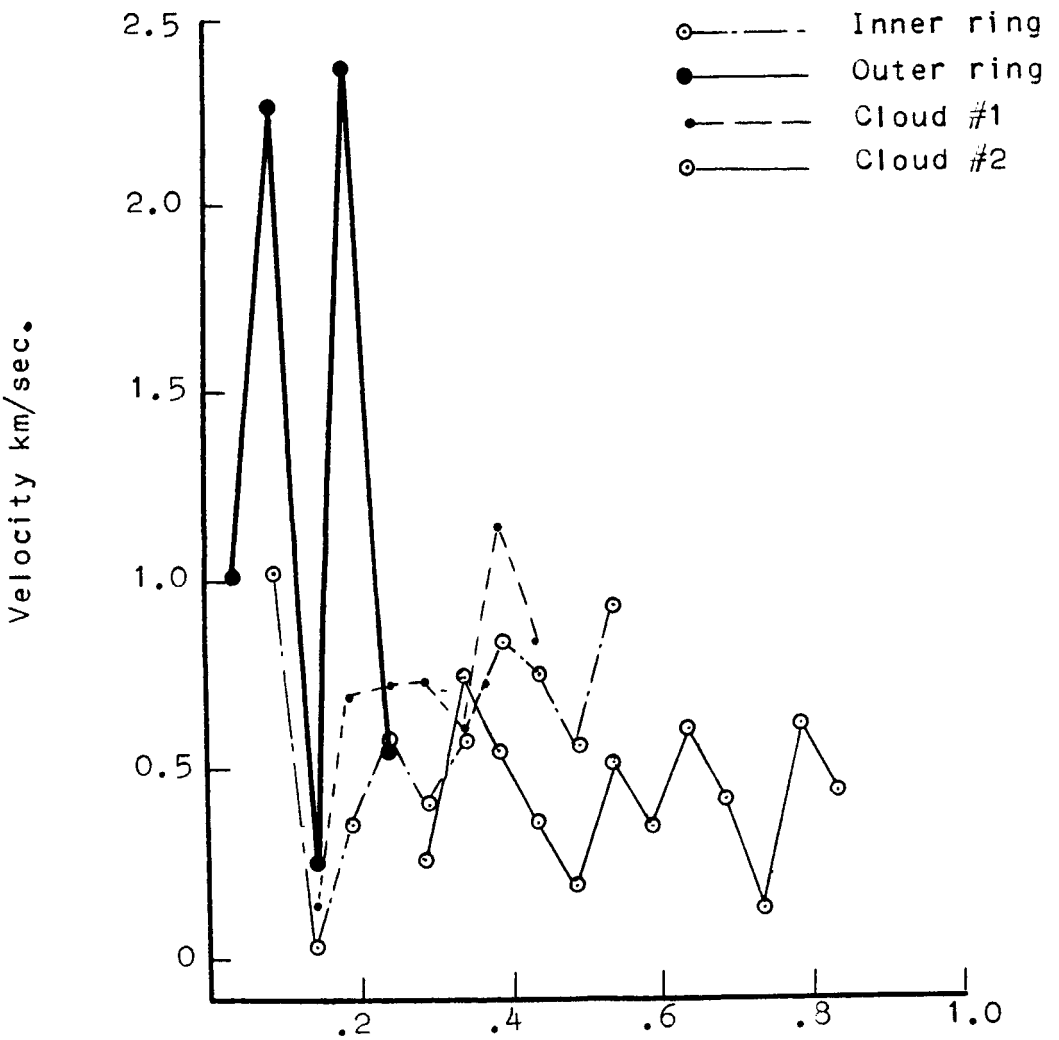

Velocity of Cloud Edges and Internal Cloudlets
(Melbourne Beach)

Figure 3.25

3.4 Expansion Rate Analysis (cont'd)

velocity calculations to be extended in time as long as those from the False Cape location. Only two of the cloudlets identified from the False Cape location could also be identified in the pictures obtained from the Melbourne Beach locations.

Velocity values for the cloudlets obtained from False Cape and Melbourne Beach can be combined at particular times to provide a true radial velocity of the cloudlets. These radial velocity values are shown in Figure 3.26. The resulting smoothing out of the velocity fluctuations is significant. It indicates the degree to which turbulence affected the cloudlet motion.

During the time that cloudlets number one and two could be measured the average velocity of each varied in opposite manners. The average radial velocity of cloudlet number one increased while that of cloudlet number two decreased. However, cloudlet number two was observed for slightly longer than one-half a second more than cloudlet number one. If only the first four velocity measurement values for cloudlet number two are considered, these overlap the time when velocity values for cloudlet number one were obtained, and an increase in velocity of cloudlet number two with time results.

There may be a critical time, slightly less than 0.5 second, during which the pressure within the cloud is enhanced due to the evaporation of the liquid droplets.

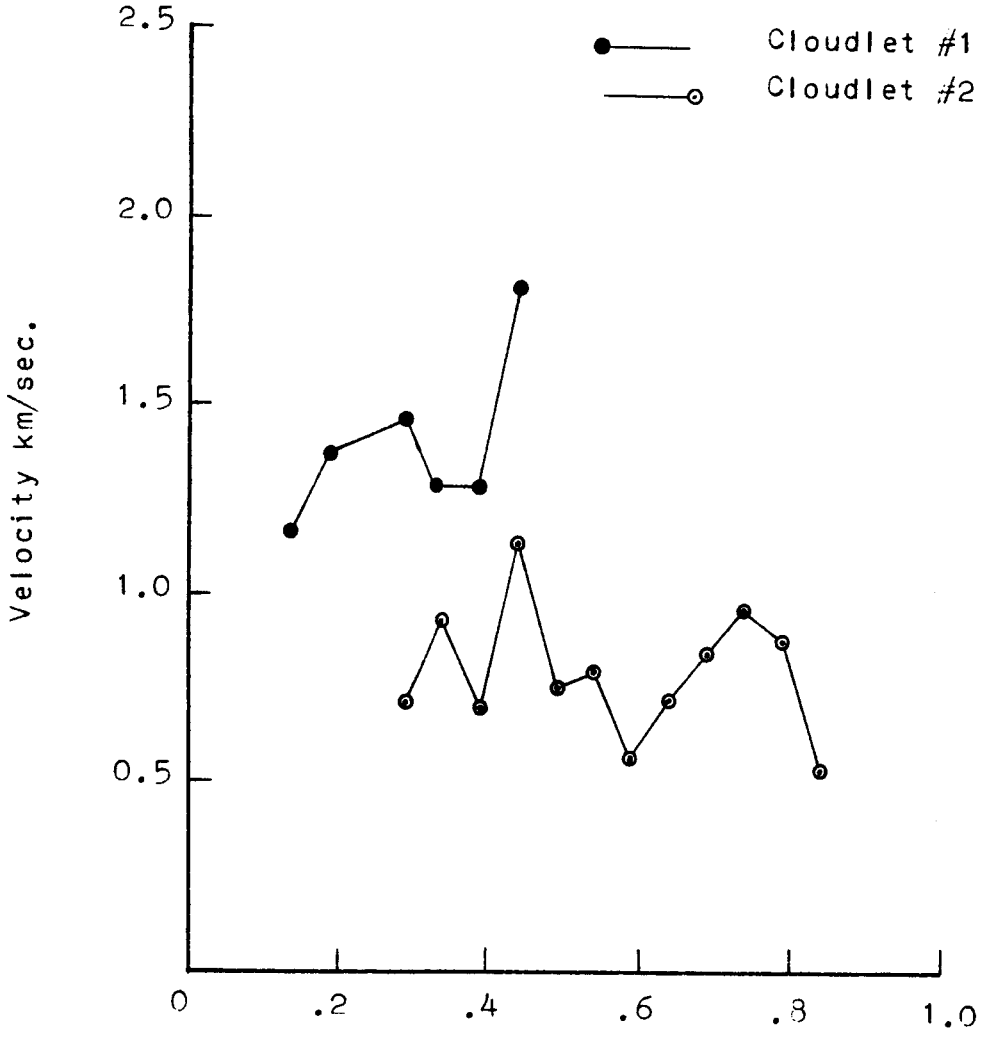

Radial Velocity of Cloudlets

Figure 3.26

3.4 Expansion Rate Analysis (cont'd)

After this period of time condensation occurs and the pressure drops more rapidly, resulting in the observed decrease in velocity of the cloudlets. This process of evaporation-condensation-sublimation was found to exist in laboratory experiments of the release of liquids at ionospheric pressure (Ref. 6 and 9).

4.0 Radiofrequency Electromagnetic Observations

A variety of radiofrequency electromagnetic observations were made in conjunction with Project High Water I. The following sets of data from these observations were made available for this analysis effort:

1. Ionosonde observations acquired at Cape Kennedy and Grand Bahama Island,
2. Electromagnetic noise observations acquired with receivers located at Patrick Air Force Base (Florida) Technical Laboratory, of frequencies of 232.36 mc/sec, 136.2 mc/sec, and 13.820 mc/sec.,
3. Telemetry signal intensities recorded at Cape Tel. II, at telemetry channel frequencies of 242.0 mc/sec, 246.3 mc/sec, 248.6 mc/sec, and 249.9 mc/sec,
4. Noise measurements at 15 kc/sec and the strength of 18 kc/sec WWV carrier (obtained by switching a (Empire Devices Model NF-105) noise and field

intensity meter between the two modes), continuous record of the signal level observed with a (PRM-1) Stoddard receiver (The Noise and Field Intensity Meter, and the Stoddard Receiver were operated by Martin personnel and were located on Martin-Orlando property.),

5. A static direction finder system, tuned to 10 kc/sec, operated by weather detachments located at Patrick Air Force Base (Florida), and at Andrews Air Force Base (Maryland).

A number of additional observations are believed to have been made, but it has not been possible to ascertain the disposition of the pertinent records.

Since the nature and the interpretation of the various observations differ considerably, a brief discussion of each of the above categories will be presented.

4.1 Ionosonde Observations

J. W. Wright (Chief, Vertical Soundings, Ionosphere Research and Propagation Division, National Bureau of Standards, Boulder, Colorado) gave the following description of the ionospheric conditions (Ref. 8):

Pre-Release

A "Sporadic E" layer (E_s) at a altitude of 107 $\pm$ 2 km was embedded in the normal E layer. This E_s is definitely

4.1 Ionosonde Observations (cont'd)

believed to have covered the area of release, since it was observed at both Cape Kennedy ($f_o E_s$ = 6.0 mc/sec) and at Grand Bahama Island ($f_o E_s$ = 3.9 mc/sec). There was evidence of a traveling disturbance in the F-region; however, the E_s at Cape Kennedy obscured reflections from the F-region.

Post-Release

No significant changes in the E-region were observed at either station at or following the water release. Minor changes in the E-region were observed. These minor changes noted were:

(A) At the moment of release, the decreasing trend in the value of the critical frequency (f_o) of the E_s layer was arrested, and the $f_o E_s$ remained constant for at least thirty-five (35) minutes.

(B) A slightly unusual "E_s" stratum at an altitude of 90 km was observed at Cape Kennedy, beginning about thirteen minutes after the release, and continuing for at least eleven (11) minutes.

In this analysis, both of the preceding minor changes in the E-region of the ionosphere are considered to be direct consequences of the water release. These two changes (in the E-region) are results of the combined effects of phenomena associated with the release of water.

4.1 Ionosonde Observations (cont'd)

There are two effects of the water release which contribute to the arrest of the decreasing trend in the critical frequency of the E_s layer ($f_o E_s$). These effects are:

(a) The release of water created a disturbance or perturbation wave, which propagated radially from the release point with a velocity equal to the initial expansion velocity of the water i.e., 2.5 - 3 km/sec. This propagation velocity remained constant, but the amplitude of the wave decreased with distance. Therefore, the perturbation wave reached Cape Kennedy in 35-40 seconds after the release.

(b) The release of the water altered the motion of the "ionospheric cloud" producing the E_s anomaly.

The perturbation wave and the presence of the water in the ionosphere can be expected to alter the electron gradient and the change in the electron gradient with time. The arresting of the trend in $f_o E_s$ for thirty five (35) minutes graphically demonstrates the magnitude of disturbance created by the water release.

The slightly unusual "E_s" stratum at an altitude of 90 k is considered in this analysis to be a consequence of the arrival of the water vapor over the Cape Kennedy area. The

4.1 Ionosonde Observations (cont'd)

physical movement of the water-vapor can be expected to follow an exponential decay in velocity, since the primary driving force was generated at the release. If the initial expansion velocity is taken to be 3 km/sec., the exponential velocity behavior predicts that the vapor cloud will, as a consequence of the "self-contained" expansive force, expand to a diameter of about 50 km. (Expansion beyond the 50 km diameter will be as a consequence of diffusional effects.) However, the expansion will not be spherically symmetrical, since the expanding vapor cloud will encounter the denser atmosphere below. The expansion of the vapor cloud will be superimposed on the existing ionospheric motion. Considering these factors, the slightly unusual E_s - stratum indicates that there was an ionospheric wind at an altitude of 90 km from the southeast with a velocity of 76 m/sec. An ionospheric wind velocity of 76 m/sec. is in excellent agreement with a passage time of eleven (11) minutes for the vapor cloud.

The generation of a disturbance or perturbation wave with the release of water at a pressure of 10^{-4} torr has been experimentally observed (Ref. 9). It is also noted that it was widely held that Project High Water I release would not produce significant changes in the ionosphere (Ref. 2). The ionosonde observations are considered to be a confirmation of the scale model laboratory studies and that detectable effects would be produced in the ionosphere.

4.2 Electromagnetic Noise Observations

Electromagnetic noise observations were made at Patrick Air Force Base at 232.36 mc/sec, 136.2 mc/sec, and 13.820 mc/sec. (Ref. 11). (The bandwidth of the receivers was 16 kc/sec.). Initiation of the observations was at approximately lift-off of the vehicle (1400:32Z), and continued until approximately five (5) minutes after the release (1408+Z).

The 232.36 mc/sec records demonstrated only minor fluctuations (maximum relative amplitude: 6-7 units) except during the time the vehicle was in the pattern of the antenna. A sustained signal was observed which ceased upon the destruct of the vehicle (or release of the water). Evidently the sustained signal was generated by some electronic system aboard the vehicle. Following the release, a number of sharp spikes in the signal level were recorded. The intensity and relative occurrence of these sharp spikes decreased rapidly after twenty-one (21) seconds from the time of the release.

The records of the observations at 136.2 mc/sec were very similar to the 232.36 mc/sec records; however, no sustained signal was received at 136.2 mc/sec as was observed at 232.36 mc/sec. A lone sharp spike (relative amplitude: 15 units) was recorded about four (4) seconds prior to the release, otherwise the amplitude variations were small (relative amplitude: 6-7 units). A similar pattern of sharp spikes in signal amplitude followed the water release and also decreased in amplitude and relative occurrence after

4.2 Electromagnetic Noise Observations (cont'd)

twenty one (21) seconds.

The records for the observations at 13.820 mc/sec differ considerably from those for the above frequencies. A considerable variation in the background level occurred. There appeared to be both a short term and a long term cyclic variation in the observed signals, both before and after the water release. Although a number of sharp spikes in the signal amplitude were recorded prior to the water release, the relative density of the spikes increased for twenty one (21) seconds following the water release. A general change in the observed signal pattern occurred approximately three (3) seconds after the water release and persisted until about twenty (20) seconds after the water release. A peculiar set of signals was recorded from forty-two (42) seconds to fifty (50) seconds following the water release.

These noise measurements made at Patrick Air Force Base clearly demonstrate that an increase in electrical activity developed following the water release. A detailed examination was made of the noise observation records to ascertain the degrees of coordination between the sharp amplitude variations. A total of twenty-seven (27) spikes were simultaneously recorded on all three (3) records. The relative amplitudes of these coordinated signal fluctuations are summarized in Table 4.1. A large number of additional

TABLE 4.1

Relative Amplitude of Noise Observations

UT	RT	Rel. Amp. 232.6mc/sec.	Rel. Amp. 136.2mc/sec.	Rel. Amp. 13.820mc/sec.	Total Rel. Amp.
1403:16.75	162.75	5.5	16.0	1.0	4.0
:17.0	163.0	5.5	15.0	2.0	5.5
:19.50	165.5	3.0	16.0	1.0	5.0
:22.25	168.25	18.0	35.0	2.5	9.5
:26.0+	172.0+	21.0	37.0	13.0	17.5
:26.5	172.5	4.0	23.0	1.8	6.8
:31.25	177.25	8.0	31.0	3.0	8.0
:31.75	177.75	9.0	27.2	2.0	7.0
:36.50	182.5	15.0	25.5	0.5	5.0
:38.50	184.5	12.0	8.2	4.0	5.9
1404:02.0	210.0	7.0	4.0	8.0	8.0
:02.5	210.5	10.0	8.0	5.0	5.0
:05.50	213.5	17.0	12.5	2.0	6.8
:06.0	214.0	8.0	7.0	4.0	9.0
:47.75	255.75	5.0	19.0	2.8	4.8
1405:40.75	308.75	5.0	17.5	10.0	10.0
1406:04.5	332.5	9.0	22.0	2.5	2.5
:13.5	341.5	5.0	28.0	4.8	4.8
:32.5	360.5	7.0	35.0	3.0	5.0
:33.0	361.0	6.5	10.0	4.0	6.0
:36.0	364.0	7.0	7.0	15.0	20.0
:40.75	368.75	15.0	35.0	5.0	12.0
:43.50	371.50	12.5	8.0	13.0	20.0
:44.75	372.5	3.0	19.0	3.0	4.0
:49.0	377.0	6.5	31.5	6.0	10.0
:49.75	377.75	10.5	25.8	10.0	17.0
:49.75+	377.75+	8.0	24.0	3.0	12.0

4.2 Electromagnetic Noise Observations (cont'd)

amplitude spikes were observed in the individual records which did not show a correlation on all three records. No correlations were observed beyond 1406:50Z. In a number of instances amplitude spikes were simultaneously observed on two (2) of the three (3) records. In general, there was a better correlation between the 232.36 mc/sec and the 136.2 mc/sec records; however, there were a few instances where there was a correlation between the 13.820 mc/sec amplitude spikes and spikes on one of the other records.

There is considerable doubt that "lightning-like" electrical discharges (or electrical "strokes") were responsible for the generation of the amplitude spikes. The only possible exception is the amplitude spikes recorded at 1403:26+Z. This particular set of spikes occurred very close to the time the ice-cloud dissipated. Although the evidence is not conclusive, it is believed that the electrical effects following the water release were more akin to the electrical disturbance observed during the turbulent development of a cumulo-congestus cloud. That is, the electrical effects are a consequence of acceleration (and/or deceleration) of electrical charges rather than of actual electrical discharges. There is ample reason to believe that charge separation occurred (See Appendix D) in the water-ice-vapor cloud, but evidence in favor of an actual electrical discharge is lacking.

4.3 Telemetry Signal Level Records

Telemetry signal level records were examined in the hope that telemetry transmission continued beyond the time of the water release, as was observed in Project High Water II (Ref. 6). It was found, however, that all telemetry systems ceased transmitting at the time of the water release.

The telemetry signal level records did reveal a number of attenuations superimposed upon the expected signal attenuation with range. The signal attenuations were briefly reviewed and a rather remarkable correlation was found between the altitudes of the telemetry attenuations and the altitudes at which discrete changes in ELF-VLF spectral observations were recorded (ISC Summary Report). In particular, it was found that at every altitude where ELF-VLF spectral observations displayed distinctive variations in attenuation, these phenomena also occurred in the telemetry signal levels. In addition, a number of vehicle events can be identified from the telemetry signal level variations in a manner similar to those employed in ELF-VLF spectral data interpretations. It is remarked that ELF-VLF spectral observations provide more distinctive and detailed information concerning the altitude regimes and vehicular events than the telemetry signal level records yield. Furthermore, it is emphasized that the ELF-VLF spectral methods for identifying altitude regimes and

4.3 Telemetry Signal Level Records (cont'd)

vehicle events were developed completely independently of telemetry considerations (Ref. 12,13,14,15).

A comparison of the attenuations which occurred at each of the frequencies reveals that the extent of the attenuation is frequency dependent in a number of instances. In those instances where the attenuation is more or less independent of the frequency, the attenuation is probably primarily the result of refractive effects. On the other hand, attenuations which are frequency dependent are believed to be primarily a consequence of signal absorption (Ref. 16).

A cross correlation between the telemetry signal attenuations and corresponding ELF spectral observations will establish the cause of the observed telemetry attenuations and will assist in establishing procedures for reducing attenuations of telemetry transmission. This dual frequency range approach is recommended as an efficient method for the development of improved telemetry and communications procedures.

4.4 Noise and Field Intensity Measurements

Observations were conducted by personnel of Martin Company at Orlando during High Water I Experiment, employing an Empire Devices, Inc., model NF-105 Noise and Field Intensity Meter. This instrument was alternated between two operational modes during the test. Mode I recorded a

4.4 Noise and Field Intensity Measurements (cont'd)

quiet 3 kc/sec band centered at 15 kc/sec, and Mode II recorded the strength of the 18 kc/sec WWV carrier. The data for Mode I (reported by Mr. Wm. Clarke) are given in Table 4.2 for the noise at 15 kc/sec and the signal strengths of the 18 kc/sec WWV carrier are recorded in Table 4.3 (Ref. 17).

TABLE 4.2

Amplitude of 3 kc/sec band centered at 15 kc/sec

Universal Time	Signal Level db above 1 v/meter/mc/sec	
1400Z	114	
1401	114	
1402	118	(bias error estimated
1403	132	to be ± 2db.
1404	147	Reading accuracy ± 1db.)
1405	147	
1406	115	
1407	114	

It was reported that the signal amplitudes at 15 kc/sec remained constant at 114 v/m/mc/sec for an additional five (5) minutes after 1407Z (the instrument was turned off at 1412Z), and that a number of "spikes in the signal strength" of the 18 kc/sec WWV carrier were "observed during the period of elevated signal."

TABLE 4.3

Signal strength of 18 kc/sec WWV carrier
(36 in loop antenna)

Universal Time	Signal Strength db above 1 v/meter
1400Z	39
1401	39
1402	39
1403	43
1404	45
1405	45
1406	39
1407	39

Unfortunately, the reported data, which was obtained by visual observation, lacks sufficient detail to permit a detailed correlation with the data recorded at Patrick Air Force Base. However, there are certain aspects which appear pertinent. It is presumed that, in both the 15 kc/sec and the 18 kc/sec observations, the increase in the signal levels reported for 1403Z occurred after the water release (1403:16.6Z). Otherwise, a considerable revision of the interpretation would be required.

The increase in the signal level at 15 kc/sec from 114 db at 1401Z to 118 db at 1402Z may or may not be significant. A portion of this increase may be due to

4.4 Noise and Field Intensity Measurements (cont'd)

the transit of the vehicle through a non-uniform lower ionosphere (HW II). The increases from 118 db at 1402Z, to 132 db at 1403Z, and then to 147 db at 1404Z, were in accordance with expectations, based on the noise recordings obtained at Patrick Air Force Base, since it was evident that the water release was accompanied with an increased electrical activity. It is believed that the persistence of the elevated signal (until at least 1405 but not until 1406Z) for a longer time than observed earlier in the 13.820 mc/sec to 232.36 mc/sec.frequency range is best explained by the acceleration or deceleration of charges. The noted time interval does provide an approximation for the time during which the vapor cloud was expanding as a consequence of the internal "expansive forces."

It is noted that no "signal spikes" were reported for the 15 kc/sec observations. If there actually were no spikes, this fact is additional support for the concept that no actual electrical discharges followed the water release.

Amplitude variations of the 18 kc/sec WWV carrier between 1402Z and 1406Z are considered to be a consequence of the "reflection" of the signals from the expanding vapor cloud. Due to the lack of timing information, there is no way to ascertain whether the reported "spikes in the signal"

4.4 Noise and Field Intensity Measurements (cont'd)

correlate with those observed in the 232.46 mc/sec to 13.320 mc/sec frequency range. This lack of information is particularly unfortunate since it would have provided further information relevant to the occurrence of electrical discharges.

Martin-Orlando employees William Clarke, Charles W. North, and William Raymond monitored the test with a Stoddard receiver, Model PRM 1. A continuous recording of the observed signals was made with this instrument from approximately 1342Z to 1431+Z. It is noted that the receiver gain was increased just after 1414Z.

The Stoddard receiver records show little resemblance to the other passive observations. Prior to vehicle lift-off, the amplitude of the recorded signal varied widely but relatively few sharp changes in the signal level were recorded. Just prior to lift-off, an increase in the signal level was initiated. The level continued to increase until shortly after lift off. Then a decreasing trend developed, followed by alternating periods of increasing and decreasing signal levels. The observed signal level variations show some correlations with the telemetry signal amplitudes, but the correlations are so poor that little significance can be attached to the comparison.

No significant variation in signal level was observed

4.4 Noise and Field Intensity Measurements (cont'd)

at the time of the water release, although a decreasing trend in the signal level was briefly halted. One possibly significant fact was noted in this record; just prior to 1406Z an unusually sharp drop in the signal level occurred. After 1406Z the signal level decreased to a minimum value and, except for brief periods, remained at this level until the receiver gain was increased at 1414Z. No significance of the signal behavior after 1406Z has been established.

4.5 Static Direction Finder System

The static direction finder system searched for pulses (at 10 kc/sec) received simultaneously at Patrick Air Force Base and at Andrews Air Force Base, and only those pulses which were received within 0.02 seconds of each other were considered valid. A single such coincidence was reported at about 18 seconds (1406:18Z) after the water release (Johnson). The bearing of the signal was about 81° from Patrick Air Force Base and the range was 30-40 miles (triangulation method). A diligent search of the noise records in the vicinity of 1406:18Z failed to yield even a minor fluctuation in the signal levels. A check was also made at T + 181 seconds range time, but only negative results were obtained. This lack of correlation of the 10 kc/sec bursts with the higher frequency data strongly suggests that the observed pulse(s) were not the consequence

4.5 Static Direction Finder System (cont'd)

of an electrical discharge. It would have been surprising if an electrical discharge had occurred some 175 seconds after the condensed phases of water disappeared.

5.0 Conclusions

Release of a liquid into the upper reaches of the atmosphere initiates a complex interdependent series of physical and chemical processes. Laboratory simulation studies permit the determination and evaluation of certain aspects of such a release; however, it is doubtful that laboratory experiments can possibly produce even a gross approximation to real ionospheric conditions. The ejection of liquids into the upper atmosphere is feasible with a number of advanced space explorations systems. Project High Water provided the first large scale investigation of the effects of releasing liquids into the ionosphere. Studies of the data acquired during Project High Water graphically illustrate the complexity of the phenomena associated with such a release. The absolute necessity of carefully integrated experiment design, adequate instrumentation, and, coordination of all factors in the analysis were also clearly demonstrated. It was discovered that the effects are so interdependent that the various aspects can not be successfully analyzed independently of each other.

As might be expected, the results of Project High Water reveal significant implications beyond the stated objectives of the program. Some of the more important implications discovered are included in this summary.

5.1 Model of Liquid Release in Space

Results from the two High Water experiments and from laboratory experiments (Ref. 9) show a definite model for the physical processes that occur when liquids are released into a region of reduced pressure.

Two critical factors involved in determining the physical processes involved are:

1. The temperatures of the released material, and
2. The difference between the vapor pressure and the actual external pressure.

From basic physics, the boiling point of a liquid is the temperature at which the vapor pressure of the liquid is equal to the external pressure (Ref. 18). When the vapor pressure exceeds the external pressure, the liquid immediately starts boiling. Since boiling generates vapor, the vapor pressure in the vicinity of the liquid (within the cloud) increases rapidly with time. This change in phase produces a correspondingly rapid reduction in the liquid temperature. This cooling causes the liquid droplets to freeze at rates which are functions of the droplet diameters (Ref. 19). The internal temperature of a frozen droplet changes comparatively slowly because the heat conduction is poor in the solid state. At these reduced temperatures, the saturation vapor pressure of the super-cooled droplets is greater than the saturation vapor pressure of a frozen particle at the same temperature (Ref. 20). Following such

5.1 Model of Liquid Release in Space (cont'd)

an explosive boiling regime, the ice particles are surrounded by environmental vapor pressures greater than their own saturation vapor pressures. Therefore, condensation from the gaseous to the solid state occurs, and the ice particles grow at the expense of the surrounding vapor. Also, as the ice particles grow, the entire cloud continues to expand, resulting in a continuously decreasing environmental vapor pressure. The vapor pressure of the system decreases until the particles experience pressures below their saturation vapor pressures. The particles then sublime directly to the vapor state.

The initial physical conditions described above were evident in the High Water I data. During the first 400 milliseconds following the release, the released water was boiling and cloud particles were accelerating outward. As the ice particles formed, the cloud acceleration decreased with time. At the same time, the original boiling generated violent dynamic conditions within the cloud. The resulting internal turbulence tended to mask the increases and decreases in radial accelerations. By combining data from two locations some of the turbulence effects can be eliminated and the radial acceleration components can be observed more clearly. Data from the High Water II test was not acquired for a sufficient length of time to determine the effects of freezing on the cloud motion.

5.1 Model of Liquid Release in Space (cont'd)

Laboratory experiments have shown that liquids released at very low pressures follow the above described regime of physical processes (Ref. 9). Laboratory experiments have disclosed evidence of a perturbation wave that travels outward with the velocity of the initial liquid expansion. The fact that retardation of the ionospheric E_s condition was observed at the time of the water release is considered to be evidence of such a perturbation.

Maximum expansion velocities of the ice-water cloud for the High Water I and the High Water II experiments are shown in Table 5.1.

TABLE 5.1

Maximum Expansion Rate of Ice-Water Cloud

Structure	High Water I* (km/sec)	High Water II** (km/sec)
Sideward Spike	2.53	3.60
General Cloud	1.83	1.83
Cloudlet	1.83	1.83

* 105 km above sea level
** 165 km above sea level

Two facts must be considered in comparing the expansion velocities of the two clouds. These facts are:

1. In High Water i, the 44,000 kg of water in the second stage, in addition to the quantity that escaped through the ports in the third stage, was released suddenly, while in High Water II the

the entire 86,000 kg of water was suddenly released.

2. The ambient conditions into which the water was released were quite different in the two experiments, as shown in Table 5.2 (Ref. 21).

TABLE 5.2

Atmospheric Properties

Altitude	Pressure (mm Hg)	Number Density (n/m^3)	Molecular Weight
105	10^{-4}	5×10^{18}	28.85
165	2.5×10^{-6}	2×10^{16}	27.90

Consideration of these facts explains why the water released at 165 km dissipated much more rapidly than that released at 105 km. This result was observed when data from the two operations were compared. The cloud formed in High Water I required about ten (10) seconds to optically disappear, while the High Water II cloud was visible for only approximately five (5) seconds.

Results from the High Water experiments raises grave doubts of theories proposing the existence of accumulations of ice in space. For any quantity of ice to exist, one of two improbable conditions would be required: 1) extremely low ambient temperature at the space location when the formation occurred, or, 2) formation in a high gravity environment, followed by cooling to an extremely low temperature prior to release to a low pressure environment.

5.1 Model of Liquid Release in Space (cont'd)

Three particular theories of types of "ice in space" to which Project High Water data are directly applicable are:

1. Noctilucent clouds,
2. Ice on the moon,
3. Ice theory of comets.

Noctilucent clouds are rare, cirrus-like, silvery clouds which have been observed at heights as great as 82 km (Ref. 22). These clouds occur at high latitudes and are visible only after sundown but while the cloud is still in the sunlight. One of the proposed explanations for these clouds is that they are composed of ice particles. Since the ambient pressure at an altitude of 82 km is of the order of 6×10^{-3} mm Hg (Ref. 21), the maximum temperature possible for the existence of ice particles (i.e., the sublimation temperature) is about $-60^{\circ}C(213^{\circ}K)$. Although the freezing temperature of particles is size dependent, the minimum temperature at which supercooled water can exist is about -40° ($233^{\circ}K$). Accordingly, the most probable mode of formation of an ice particle at 82 km altitude is by direct condensation from the vapor state to the solid state. At 82 km, the kinetic temperature is $-107^{\circ}C(166^{\circ}K)$. (Ref. 21). Therefore, if the total ambient pressure were due to water vapor, one gram of water vapor would occupy a volume of 1000 M^3. The partial pressure of water at 82 km is probably

5.1 Model of Liquid Release in Space (cont'd)

no greater than 10^{-4} mm of Hg, therefore, the volume involved is probably in excess of 60,000 M^3. With a mean free path of the order of 10^{-3}M, the accumulation of an appreciable amount of water (ice) at any one location would be extremely difficult. Therefore, it is concluded that, if the noctilucent clouds are composed of ice particles, these particles must be extremely minute.

It has been proposed that bulk water may exist on the moon within a porous structure (Ref. 23). Project High Water results provide particularly convincing reasons to doubt this concept. Numerous efforts have been made to evaluate the density of the lunar atmosphere. One of the widely accepted values is some 10^{-13} of the sea-level density of the earth's atmosphere (Ref. 24). It follows that the equilibrium temperature at the ambient pressure of the lunar surface is much lower than the measured temperatures existing there, and any lunar water not chemically bound would dissipate as rapidly as, and in a manner analogous to, that observed with Project High Water releases. In order for any bulk lunar water exposed to the lunar atmospheric conditions to remain for any appreciable period of time, its temperature would have to be maintained at about -150°C (123°K). The minimum observed night time temperature of the moon's surface is barely below the

5.1 Model of Liquid Release in Space (cont'd)

required value (d.h., -157°C or 116°K), while the day time temperature is very much higher (d.h., 101°C or 374°K) (Ref. 25). Even if the lunar age is taken to be less than that of the earth, the prospect of finding bulk water on the moon are considered to be remote.

A preliminary evaluation of the "ice theory on comets" (Ref. 26) has been made in view of the Project High Water experimental results. One of the important characteristics of a comet is the extraordinary tenuity (Ref. 27). The fact that the nucleus of a comet does not suffer an appreciable decrease in mass at a perihelion of 500,000 km from the sun and a surface temperature of 4500°K (Ref. 26) is, at best, difficult to explain if the one of the primary constituents is ice. The escape velocity of a water molecule from a comet would be very low (e.g., the escape velocity of a water molecule from the surface of the moon is only 2.4 km/sec (Ref. 28)). At a temperature of 50°K, the root mean square velocity of a gaseous water molecule is 0.24 km/sec (Ref. 29). Therefore, in view of the small mass of a comet, water molecules would rapidly escape from the surface of the comet nucleus. Theoretical calculations indicate that particles in the tail of a comet have radii of less than 10^{-5} cm. Even if the absorption coefficient of ice particles is only 10^{-4}, an ice particle in a comet 93,000,000 miles from the sun would absorb more than a sufficient amount of

5.1 Model of Liquid Release in Space (cont'd)

energy to vaporize it, since the solar constant (at the earth) is 1.94 cal/cm^2/min. (Ref. 30). These considerations cast considerable doubt on the "ice theory of comets." Additional experimental studie of the behavior of ice in reduced pressure environments would provide the requisite knowledge to adequately evaluate the concept of ice in comets.

5.2 Ionospheric Effects

Release of the ballast water of the Saturn vehicles produced a substantial modification of the composition of the ionosphere in the vicinity of the release. The effects of this composition change were found to be largely dissipated in a relatively short distance. This was evidenced by the fact that only a minor change was caused in the ionosonde observations performed at Cape Kennedy and at Grand Bahama Island. On the other hand, it was observed that the release produced a perturbation wave which propagated at a velocity of the order of 3 km/sec. The Project High Water data suggest that the energy content of the ionosphere may be of greater significance than its composition.

Evidence of inhomogeneities in the ionosphere has been obtained from a variety of sources. Project High Water data adds considerable evidence that ionospheric inhomogeneities are present, and that the inhomogeneities cause degradation of telemetry and radar transmissions. Such degradation of

5.2 Ionospheric Effects (cont'd)

electromagnetic signals by ionospheric inhomogeneities was especially evident in analyses of data obtained during the second release experiment (Ref. 6). A striking similarity was noted in the radar and telemetry effects observed after the SA-3 vehicle traversed the E-layer and those produced by the High Water vapor cloud inhomogeneity. This similarity is considered to be strong evidence that the observed E-layer attenuations were a consequence of inhomogeneities in the ionosphere.

5.3 Electrical Phenomena

Release of water into the ionosphere produced definite electrical effects. The electromagnetic noise observations clearly demonstrated an increased electrical activity. The bulk of the electrical activity generated appears to have been a consequence of acceleration and/or deceleration of charges. Signals that were obtained at 5.5 mc in High Water II experiment (Ref. 6), are believed to be related to the gyromagnetic motion of electrons.

No evidence was found which would support the proposal that "lightning-like" electrical discharges occurred in the water-ice-vapor cloud. On the basis of existing data, it is believed that no actual electrical discharges occurred. If so, this is a highly significant fact. Charge separation certainly was to be expected; however, it appears that the charge centers were sufficiently removed from one another that a discharge did not occur (See Appendix D).

5.4 Importance to Space Exploration

Project High Water and associated laboratory experiments have produced results that have important applications to space exploration. The problems to which these results apply can be characterized into three general areas:

1. Existence of ice in space,
2. Conditions associated with an abort,
3. Communications and telemetry problems.

In each of these areas new experimental data were obtained from the High Water project.

As described above, the fact that the High Water experiments demonstrated very rapid dissipation and disappearance of the ice clouds casts considerable doubt on theories assuming the existence of ice in space. Any quantity of ice existing in space must have been cooled (over a long period of time) to a very low temperature before the ambient pressure was reduced. Under the continual influence of radiation from the sun, the water molecules would gain energy and rapidly dissipate into space.

Conditions associated with a potential abort were demonstrated by the High Water project. If an astronaut were enveloped within the expanding cloud from an abort he would experience an environment similar to that produced by the High Water experiment. During the evaporation and sublimation regimes, the temperature of his environment

5.4 Importance to Space Exploration (cont'd)

will be suddenly and drastically reduced (Ref. 6,9). If he were outside the vehicle at the time of a release, he would experience a perturbation wave such as was evident in the laboratory experiments (Ref. 9). A similar perturbation wave appeared to be associated with the High Water I operation. The cloud resulting from an abort would also cause telemetry and radio dropouts (Ref. 6). If an abort should result in the release of fuels and oxidizers, the ensuing turbulence would produce mixing and would therefore increase the fire hazard.

Communication attenuations are caused by interaction of the electromagnetic signals with inhomogeneities in the atmosphere. Project High Water provided a synthetic inhomogeneity within the ionosphere. Unfortunately, almost no telemetry signals were received after the water release in the High Water I experiment. However, both telemetry and radar returns following the High Water II release showed the effects of the induced inhomogeneities. These effects were strikingly similar to effects that have been obtained as a launch vehicle passes through regions of the ionosphere. Thus, the High Water data appears to confirm the concept of naturally occurring inhomogeneities within the ionosphere.

5.5 Further Experiments

While the Project High Water experiments have provided some excellent direct data concerning several physical

5.5 Further Experiments (cont'd)

phenomena important to space explorations, there is a very great need for additional data. There is a particularly pressing need for data necessary to more completely analyze and understand the effects of ionospheric inhomogeneities on communications. For example, further experimentation should be designed to obtain the maximum information concerning the frequency effect of a synthetically induced inhomogeneity in the ionosphere. One approach to such an experiment is outlined below.

A series of High Water type experiments should be carried out with water releases at different altitudes. These altitudes should range from 40 km to 400 km. The same quantity of water should be released in each experiment. This aspect is essential if the various tests are to be directly comparable. For each test a telemetry pod should be released from the vehicle at a predetermined time interval before the water is released. This pod should be transmitting on at least five narrow band-width frequencies. The frequency effect of the induced inhomogeneity could then be analyzed from the resulting data. The release of the telemetry pod must be timed so that it is a distance, say D kilometers, from the vehicle when the water is released, but close enough to be enveloped by the cloud before the cloud dissipates. The optimum distance D is estimated to be approximately two (2) km, for a release of about the

5.5 Further Experiments (cont'd)

same quantity of water under the same general launch conditions as in High Water I and II experiments. The necessary physical data information concerning the environment and the change in environment can be measured from the telemetry pod.

Location of ground receiving stations is of particular importance to the above experiment. Simultaneous reception of signals is required, both of those traversing the cloud and those not traversing the cloud between the point of origin and the receiver. It is very desirable that some of the ray-paths pass through the cloud. Data acquired in this manner will provide further insight into the telemetry attenuation problem. Also, data acquired in the above described manner will provide valuable information for design of space-earth communication systems.

One of the aspects illustrated by the High Water experiments was the ability of ELF spectral data to provide information concerning the interaction between electromagnetic signals from a launch vehicle and inhomogeneities in both the lower atmosphere and the ionosphere. Thus, considerable additional valuable data concerning inhomogeneous regions in the ionosphere can be obtained by acquisition of both appropriate ELF spectral data and telemetry signals during the passage of a vehicle through the ionosphere. ELF spectral data concerned with telemetry attenuation can

5.5 Further Experiments (cont'd)

be acquired from normal NASA launches.

A program of cross-correlating ELF spectral data with telemetry data from launch operation will provide models of inhomogeneous regions in the ionosphere that produce telemetry attenuation.

APPENDICES

APPENDIX A

Ionospheric Conditions

Molecular disassociations produced by the absorption of solar ultra-violet and X-ray radiation change the chemical and physical composition of the ionosphere. Thus, the water released at different altitude levels will experience different ambient conditions. Not only does the density of the ambient atmosphere change with altitude, but the kinetic temperature and the mean molecular weight of the atmosphere also change. All of these pertinent variables must be considered in any analysis of physical phenomena in the ionosphere.

A profile of the mean conditions of the ionosphere is not sufficient to explain many of the observed phenomena. Horizontal variations in the density of the constituents may be as significant as the vertical profile. (Ref. 31). However, details of horizontal variations are very incompletely known. With this limitation in mind, some average ionospheric parameters for particular ionospheric altitudes are presented in Table A below (Ref. 21).

TABLE A

Ionospheric Parameters

Altitude (Km)	Kinetic Temp. (^{o}K)	Pressure (mmHg)	Molecular Weight	Mean Free Path (m)	Number Density (n/m^3)	Electron Density (n/m^3)
80	166	7.56^{-3}	28.97	3.80^{-3}	4.42^{+20}	1.0^{+11}
100	199	1.60^{-4}	28.90	.22	7.80^{+18}	1.5^{+11}
120	477	1.52^{-5}	28.71	5.45	3.10^{+17}	2.0^{+11}
140	850	5.63^{-6}	28.45	26.30	6.40^{+16}	2.8^{+11}
160	1207	3.01^{-6}	28.04	70.00	2.41^{+16}	3.5^{+11}
180	1371	1.88^{-6}	27.36	128.00	1.32^{+16}	5.0^{+11}

APPENDIX B

Optical Instrumentation

TABLE B (Ref. 1)

Instrument[a]	Location	Lens F.L. (in.)	Frames/sec	Film Size
IGOR	False Cape	180	30	70 mm
IGOR	Williams Point	360	30	70 mm
IGOR	Canova Beach	360	30	70 mm
IGOR	Patrick AFB	360	48	35 mm
ROTI	Melbourne Beach	400	20	70 mm
ROTI	Vero Beach	100	10	70 mm
IGOR	GBI	180	10	70 mm
M-45	West of launch site	10	24	35 mm
M-45	West of launch site	20	24	35 mm
Mitchell Camera	Vero Beach	10	24	35 mm
Mitchell Camera	Vero Beach	20	24	35 mm
Mitchell Camera	GBI	40	24	35 mm
Mitchell Camera	GBI	10	24	35 mm
Spectral Polarization Recorder	Jupiter	6	16	35 mm
Spectral Polarization Recorder	GBI	6	16	35 mm
T-11 aerographic	(3) in launch area	4	1	9 in.
Navy A3D aircraft aerial camera motion picture camera	Water release area	36	-	9 in.
	(3) in launch area	4	1	35 mm
Navy A3D aircraft aerial camera motion picture camera	Water release area	6	-	9 in.
		6	-	35 mm
U-2 aircraft (2) motion picture camera	Water release area	6	-	16 mm
Experimental aircraft motion picture camera		-	-	35 mm
KC-135 (ramp) aircraft motion picture camera		20	-	35 mm
Motion picture camera		6	-	16 mm
CF-100 (CARDE) aircraft (4) motion picture cameras		-	-	35 mm
NAVY SHIP motion picture camera	Water release area	80	48	16 mm
motion picture camera		-	-	16 mm

[a]IGOR- Intercept Ground Optical Recorder, ROTI - Recording Optical Tracking Instrument.

APPENDIX C

HYDRODYNAMICS OF EXPANDING LIQUIDS

Formulation of a theory for liquid expansion at reduced pressures can be developed from hydrodynamic-thermodynamic considerations. This approach provides an expression for the density of the expanding liquid. A number of physical parameters such as surface temperature, vapor pressure, viscosity, and initial density are relevant to the expansion. For the initial formulation of a theory for the expansion of liquids at reduced pressures, phase changes have been neglected. Future theoretical investigations should incorporate these important effects. The ability of any density expression to predict the rate of rarefaction of a specific liquid depends on the values chosen for the above-mentioned parameters.

Consider a spherical mass of fluid initially at rest in a region of zero pressure. At time t=0 the restraining membrane is instantaneously removed, allowing the fluid to expand into the evacuated region. It is assumed for reasons of simplicity that the expansion is spherically symmetric. Vaporization effects are neglected, and the expansion is considered adiabatic. Euler's equation for hydrodynamic flow is

$$\rho \frac{d^2\vec{r}}{dt^2} = \rho\vec{g} \quad \Delta P \qquad (1)$$

where

$\rho = \rho(r, t)$ density

$\vec{r}$ = position vector

$\vec{g}$ = gravitational acceleration

P = pressure of the flow

The equation of continuity from hydrodynamics is

$$\frac{\partial \rho}{\partial t} + \nabla \cdot (\rho \dot{r}) = 0 \qquad (2)$$

Equation (2) represents the flow through a volume bounded by an arbitrary surface in the flow region. Since the fluid flow is due to the expansion, it is certainly a nonequilibrium event. Therefore, equation (2) for this problem must be re-interpreted as

$$\frac{\partial \rho}{\partial t} + \nabla \cdot (\rho \dot{r}) = -k\rho \qquad (3)$$

where k is the "growth factor". Insertion of the First Law of Thermodynamics gives

$$Q = S \frac{dT}{dt} + P\frac{d(1/\rho)}{dt} \qquad (4)$$

where

Q = energy added

S = specific heat

T = absolute temperature

P = pressure of the flow

ρ = density

For an adiabatic expansion, Q=0 and equation (2) becomes

$$Q = 0 = S \frac{dT}{dt} + P \frac{d(1/\rho)}{dt} \qquad (5)$$

The divergence of a function in spherical coordinates can be expressed as

$$\nabla F = \frac{1}{r^2}\frac{\partial (r^2 F_r)}{\partial r} + \frac{1}{r \sin\phi}\frac{\partial F_\phi \sin\phi}{\partial \phi} + \frac{1}{r \sin\theta}\frac{\partial F_\theta}{\partial \theta} \qquad (6)$$

where

r = radius of a sphere

ϕ = azimuth angle

θ = elevation angle

F = function

Applying this concept in equation (2), the div(ρr) for the spherically symmetric event is

$$\nabla \cdot (\rho r) = \frac{1}{r^2}\frac{\partial (r^2 \rho \dot{r})}{\partial r} = \frac{1}{r^2}(2r\rho\dot{r}) + \frac{r^2}{r^2}\dot{r}\frac{\partial \rho}{\partial r} + \rho\frac{\partial \dot{r}}{\partial r} \qquad (7)$$

Now if $(\partial \rho)/\partial r = \rho r$ during the initial phases of the expansion, and $\partial \dot{r}/\partial r = 0$, then

$$\nabla \cdot (\rho r) = \frac{2\rho\dot{r}}{r} + \dot{r}\rho r \qquad (8)$$

Equation (2) thus becomes

$$\frac{\partial \rho}{\partial t} + \frac{2\rho\dot{r}}{\dot{r}} + \dot{r}\rho r + \rho k = 0 \qquad (9)$$

Solving equation (4) for the pressure and setting $S\frac{\partial T}{\partial t} = Z$

$$P = -\frac{Z}{\frac{d(1/\rho)}{dt}} = \frac{Z\rho^2}{\dot{\rho}} \qquad (10)$$

The gradient of a function $\underline{f}$ in spherical coordinates may be expressed as

$$\nabla f = \mu_r \frac{\partial f}{\partial r} + \mu\phi\frac{1}{r}\frac{\partial f}{\partial \phi} + \mu\theta\frac{1}{r\sin\phi}\frac{\partial f}{\partial \theta} \qquad (11)$$

where the μ's are the spherical unit vectors. Thus, the gradient of P becomes

$$\nabla P = \nabla\left(\frac{Z\rho^2}{\dot{\rho}}\right) = 2Z\rho\frac{\partial \rho}{\partial r}\dot{\rho}^{-1} - Z\rho^2\dot{\rho}^{-2}\frac{\partial \dot{\rho}}{\partial r} \qquad (12)$$

As previously $\partial\rho/\partial r = \rho r$ and $\partial\rho / \partial r = 0$. Thus,

$$\nabla P = \frac{2Z\rho^2 r}{\dot{\rho}} \qquad (13)$$

Equation (4) thus becomes

$$\frac{d^2r}{dt^2} - g = -\frac{2Z}{\rho}\rho^2 r \qquad (14)$$

Assuming the intrinsic acceleration of the expansion is constant, set

$$\frac{d^2r}{dt^2} - g = a \qquad (15)$$

Adding equations (9) and (14) produces

$$\dot{\rho}a + 2Z\,\rho r + \dot{\rho} + \frac{2\rho\dot{r}}{r} + \dot{r}\rho r + \rho k = 0 \qquad (16)$$

Applying the Bernoulli separation method and assuming the density may be represented in a product of a position function and a time function, then

$$\rho = \rho(r,\ t) = R_{(r)}\ T_{(t)} \qquad (17)$$

Substituting equation (17) in (16) yields:

$$R_{(r)}\frac{\partial T_{(t)}}{\partial t}(a) + 2Z\frac{\partial R_{(r)}}{\partial r}T_{(t)} + R_{(r)}\frac{\partial T_{(t)}}{\partial t} + \frac{2R_{(r)}\ T_{(t)}\ \dot{r}}{r} + r\ T_{(t)}\frac{\partial R_{(r)}}{\partial r} + k\ R_{(r)}\ T_{(t)} = 0 \qquad (18)$$

Dividing by R_rT_r

$$\frac{a}{T}\frac{\partial T}{\partial t} + \frac{2Z}{R}\frac{\partial R}{\partial r} + \frac{1}{T}\frac{\partial T}{\partial t} + \frac{2\dot{r}}{r} + \frac{\dot{r}}{R}\frac{\partial R}{\partial r} + k = 0 \qquad (19)$$

or

$$\frac{a}{T}\frac{\partial T}{\partial t} + \frac{1}{T}\frac{\partial T}{\partial t} + k = -\left[\frac{2Z}{R}\frac{\partial R}{\partial r} + \frac{\dot{r}}{R}\frac{\partial R}{\partial r} + \frac{2\dot{r}}{r}\right] = \mu \qquad (20)$$

Converting to total differential equations

$$\frac{1+a}{T}\frac{dT}{dt} - \mu = 0 \qquad (21)$$

$$\frac{2Z+\dot{r}}{R}\frac{dR}{dr} + \frac{2\dot{r}}{r} + k + \mu = 0 \qquad (22)$$

Solving equation (21) gives

$$T = T_o \exp \frac{\mu t}{a + 1} \tag{23}$$

and equation (22) gives

$$R = R_o \exp - \left[\frac{k(r-r_1) + (r-r_1) + 2r(\ln r - \ln r_1}{2Z + r} \right] \tag{24}$$

finally as

$$\rho = \rho (r, t) = R_{(r)} \; T_{(t)} \tag{25}$$

equations (23) and (24) must be multiplied together to give

$$\rho = \rho_o \exp \left[\frac{\mu t}{a + 1} - \frac{k(r-r_1) + \mu (r-r_1) + 2r(\ln r - \ln r_1)}{2Z - r} \right] \tag{26}$$

The expansion depends significantly on the function

$$Z = S \frac{dT}{dt} \tag{27}$$

Expansion of a liquid with a small change in temperature, (that is, with no phase change)will occur very rapidly. Conversely, high Z (rapid temperature change) implies large changes in internal energy, thus causing slower expansion.

APPENDIX D

Charge Separation Processes in Project High Water

The Project High Water experiments released water into an ionized medium (See Appendix A). Experimental studies have shown that droplets formed in the presence of charged particles become charged (Ref. 32). In the analysis of the photographic data, it was found that the maximum expansion velocity of the cloud was 1.83 km/sec. This expansion velocity is two to three times the root mean square velocity of the heavier ions present. Therefore, the initial expanding cloud would be expected to sweep out the electrons and move with a velocity exceeding the velocity of the ions. This process would result in causing the leading edge of the cloud to be negative with respect to the inner portion of the cloud. Although the physical process of evaporation is the reverse of the condensation process operative in the formation of a thunderstorm, the electrification effects in the Project High Water release are very similar to the initial electrification processes in thunderstorms (Ref. 33).

It has been experimentally demonstrated that the polarization of an insulated sphere in an electric field normally results in the deposit of appreciable free charges whenever the conductivities of the positive and negative ions are

notably different (Ref. 34). Theoretical considerations lead to an estimate of about 0.04 esu/drop, whereas the average charge measured (by aircraft) of droplets in a thunderstorm were found to be 0.11 esu/drop. Ref. 35). Since the initial expansion of the Project High Water cloud would be expected to produce charge separation, an electric field would be created. This electric field would be expected to produce further charge separation, particularly during the regrowth of the ice particles.

Potential differences were found to arise between liquid and solid phases as dilute aqueous solutions were frozen (Ref. 36). Dilute solutions of sodium chloride produced negative ice and positive water. Since the ballast water was obtained in the Cape Kennedy area, it certainly would contain sodium chloride. Thus, if any of the droplets only partially froze and the turbulent motion stripped off the water, charge separation would have occurred.

Charge separation was found to take place when rubbing contact occurred between two pieces of ice at different temperature (Ref. 37). In view of the highly turbulent motion of the Project High Water cloud, it is highly probable that rubbing contact occurred between ice particles at widely different temperatures. Therefore, it is probable that charge separation occurred as a consequence of this phenomenon.

It is evident that there were several charge separation processes which were probably operative during the expansion of the Project High Water clouds. The apparent lack of a lightning-like electrical discharge is attributed to the rapid expansion of the cloud so that the oppositely charged regions were too remote from each other for an electrical discharge to occur. Lightning discharges in thunderstorms have been observed to involve distances on the order of 600 meters between charge centers (Ref. 38).

REFERENCES

(1) K. H. Debus, W. G. Johnson, R. V. Hembree, and C. A. Lundquist, "A Preliminary Review of Upper Atmosphere Observations Made During the Saturn High Water Experiment," presented at XIII International Astronautical Congress, Sophia, Bulgaria, (September 1962).

(2) W. W. Kellogg, Memorandum to Chief, Chemistry Geophysics, and Astronomy Program, NASA, "Review of high water experiment" (February 1962).

(3) A. E. Potter, Jr. Memorandum to Aeronomy Subcommittee of the Space Science Steering Committee, "Remarks on proposal to release 200,000 lbs of water at 150 km."

(4) A. E. Potter, Jr. "Photochemistry of Saturn water release" memorandum for Kellogg Panel (February 14, 1962).

(5) H. D. Edwards, L. C. Young, and C. G. Justice "Analysis of Photographic Coverage of the Saturn SA-2 Water Experiment on April 25, 1962" Technical Report No. 1, Project A-637 (Contract NAS8-5064) NASA, Marshall Space Flight Center, Huntsville, Ala. Engineer Experiment Station, Georgia Institute of Technology, Atlanta, Ga. (September 1962).

(6) D. D. Woodbridge, J. A. Lasater, B. M. Fultz, R. E. Clark, and N. Wylie "An Analysis of the Second Project High Water Data," Report No. 02.01 (Contract NAS 10-841) NASA, Launch Operations Center, Cocoa Beach, Fla., International Space Corporation, Melbourne, Fla. (October 25, 1963).

(7) James Carter, Project High Water Tape Recording Transcription, NASA, Marshall Space Flight Center, Huntsville, Ala. (May 25, 1962).

(8) J. W. Wright, Letter report to Dr. W. G. Johnson, NASA, Marshall Space Flight Center, Huntsville, Ala. Vertical Soundings Research Section, Ionosphere Research and Propagation Division, U. S. Department of Commerce, National Bureau of Standard, Boulder Laboratories, Boulder, Colo. (May 16, 1962).

(9) D. D. Woodbridge, R. A. Knezek, and J. B. Temple "Ionospheric Water Dumping" Report No. 00.35 Vought Astronautics Division, Chance Vought Corporation, Dallas, Texas (February 5, 1962).

(10) D. D. Woodbridge and J. A. Lasater, "Unpublished Laboratory Observations," International Space Corporation.

(21) P. J. Nowrocki, and R. Papa, "Atmospheric Processes" Bedford, Mass. Geophysics Corp. of Am. (1961).

(22) W. J. Humphreys, "Physics of the Air" New York, McGraw-Hill Book Co. (1940).

(23) V. A. Firsoff, The Strange World of the Moon, New York: Basic Books (1959).

(24) C. H. Constain, B. Elsmore, and G. R. Whitfield, "Radio Observations of a Lunar Occultation of the Crab Nebula," Monthly Notices of the Royal Astronomical Society, 116 (No. 4), (1956).

(25) P. Moor, A Guide to the Planets, p 90 New York: W. W. Norton Co. (1960).

(26) O. Struve, B. Lynds, and H. Pellons, Elementary Astronomy, p 148-157, New York: Oxford Univ. Press (1959).

(27) L. Rudoux and G. de Vawcoulluevs, Larousse Encyclopedia of Astronomy, p 229-243, New York: Prometheus Press (1959).

(28) G. P. Sutton, Rocket Propulsion Elements, p 135, New York: John Wiley and Sons, Inc. (1963).

(29) S. Glasstone, Physical Chemistry, p 244-268, New York: D. Van Nostrand Co., Inc. (1946).

(30) E. W. Hewson and R. W. Langley, Meteorology Theoretical and Applied, p 73, New York: John Wiley and Sons, Inc. (1944).

(31) D. D. Woodbridge, "Physics of the Atmosphere and Space" New York: Prentice-Hall (In preparation).

(32) G. G. Goyer and G. S. Handler "Water-Vapor Condensation as a Cloud-droplet Charging Mechanism," Journal of Meteorology, 12, 569-570 (1955).

(33) R. Gunn, "Initial Electrification Processes in Thunderstorms," Journal of Meteorology, 13, 21-29 (1956).

(34) B. B. Phillips and R. Gunn, "Measurements of the Electrification of Spheres by Moving Ionized Air," Journal of Meteorology, 11, 348-351 (1954).

(35) R. Gunn, "The Hyperelectronification of Raindrops by Atmospheric Electric Fields," Journal of Meteorology, 13, 283-288 (1956).

(36) E. J. Workman and S. E. Reynolds, "Electrical phenomena occurring during the freezing of dilute aqueous solutions and their possible relationship to thunderstorm electricity," Physical Review, 78, 254-259 (1942).

(37) S. E. Reynolds, M. Brook, and M. F. Gourley, "Thunderstorm Charge Separation," Journal of Meteorology 14, 426-436 (1957).

(38) S. E. Reynolds and W. H. Neill, "The Distribution and Discharge Centers of Thunderstorm Charge Centers," Journal of Meteorology 12, 1-12 (1955).